Award Number: W81XWH-07-1-0215

TITLE: Cellular Therapy to Obtain Rapid Endochondral Bone Formation

PRINCIPAL INVESTIGATOR: Elizabeth A. Olmsted-Davis, Ph.D.

CONTRACTING ORGANIZATION: Baylor College of Medicine
Houston, TX 77030

REPORT DATE: February 2009

TYPE OF REPORT: Final Year 2

PREPARED FOR: U.S. Army Medical Research and Materiel Command
Fort Detrick, Maryland 21702-5012

REPORT DOCUMENTATION PAGE

Form Approved
OMB No. 0704-0188

1. REPORT DATE
01-02-2009

2. REPORT TYPE
Final

3. DATES COVERED
1 Jan 2007 – 28 Jan 2009

4. TITLE AND SUBTITLE

Cellular Therapy to Obtain Rapid Endochondral Bone Formation

5a. CONTRACT NUMBER

5b. GRANT NUMBER
W81XWH-07-1-0215

5c. PROGRAM ELEMENT NUMBER

6. AUTHOR(S)

Elizabeth A. Olmsted-Davis, Ph.D., Alan R. Davis, Ph.D., Michael Heggeness M.D., Jennifer West, Ph.D., Francis Gannon M.D., John Hipp, Ph.D., Ronke Olabisi Ph.D., Mary Dickinson Ph.D.,and Aya Wada, Ph.D.,

Email: edavis@bcm.tmc.edu

5d. PROJECT NUMBER

5e. TASK NUMBER

5f. WORK UNIT NUMBER

7. PERFORMING ORGANIZATION NAME(S) AND ADDRESS(ES)

Baylor College of Medicine
Houston, TX 77030

8. PERFORMING ORGANIZATION REPORT NUMBER

9. SPONSORING / MONITORING AGENCY NAME(S) AND ADDRESS(ES)
U.S. Army Medical Research and Materiel Command
Fort Detrick, Maryland 21702-5012

10. SPONSOR/MONITOR'S ACRONYM(S)

11. SPONSOR/MONITOR'S REPORT NUMBER(S)

12. DISTRIBUTION / AVAILABILITY STATEMENT
Approved for Public Release; Distribution Unlimited

13. SUPPLEMENTARY NOTES

14. ABSTRACT The goal of this study is to provide a safe effective system for inducing bone formation for fracture healing in situations of significant trauma. This set of proposed experiments will provide significant knowledge to the field of bone tissue engineering. Proposed studies will provide essential biological information and involves the development of a novel biomaterial that can safely house the cells expressing the bone inductive factor to produce the new bone at which time the material is then selectively eliminated. Ultimately this system has significant applicability. Often bone graft must be surgically removed from the pelvis, to implant into the site of difficult fractures for proper healing. This additional surgery often results in significant pain, and long term healing. Further, this system would be applicable to orthopedic trauma situations that previously resulted in amputation. We propose in these studies to complete the development of this bone induction system and test it in a preclinical animal model. Validation of our hypothesis will provide a safe and efficacious material for the production of bone leading to reliable fracture healing, circumventing the need for bone grafts, or for direct administration of cells, viruses, or other materials that could lead to significant adverse reactions.

15. SUBJECT TERMS
Not Provided

16. SECURITY CLASSIFICATION OF:			17. LIMITATION OF ABSTRACT	18. NUMBER OF PAGES	19a. NAME OF RESPONSIBLE PERSON USAMRMC
a. REPORT U	b. ABSTRACT U	c. THIS PAGE U	UU	60	19b. TELEPHONE NUMBER *(include area code)*

Standard Form 298 (Rev. 8-98)
Prescribed by ANSI Std. Z39.18

Table of Contents

Introduction: This project, on the use of cell-based gene therapy for the production of rapid endochondral bone formation, and fracture healing is a collaborative effort between a bio-engineering/biomaterials group at Rice University and Baylor College of Medicine. Although bone possesses the rare capacity to continually renew and repair itself, more than 500,000 bone repair surgical procedures are performed annually within the United States alone. The need to enhance or initiate bone formation in a controlled clinical manner has brought tissue engineering to the forefront of orthopedic research. Much recent effort has been directed to the identification of factors essential to normal bone formation, and the development of new osteoconductive materials that can temporarily fill areas of missing osteoid. Still lacking are effective osteoinductive components that could be seeded into the osteoconductive materials to generate normal bone which this study will explore. The central hypothesis of this application is that rapid bone formation can be successfully achieved with only minimally invasive percutaneous techniques and without a scaffold, by using cells transduced with adenovirus vectors to express an osteoinductive factor (BMP2), which have been encapsulated in hydrogel material and later photopolymerized at the desired site.

The goal of this study is to provide a safe effective system for inducing bone formation for fracture healing. This set of proposed experiments will provide significant knowledge to the field of bone tissue engineering. Proposed studies will provide essential biological information and involves the development of a novel biomaterial that can safely house the cells expressing the bone inductive factor to produce the new bone at which time the material is then selectively eliminated. Ultimately this system has significant applicability. Often bone graft must be surgically removed from the pelvis, to implant into the site of difficult fractures for proper healing. This additional surgery often results in significant pain, and long term healing. Further, this system would be applicable to orthopedic trauma situations that previously resulted in amputation. We propose in these studies to complete the development of this bone induction system and test it in a preclinical animal model. Validation of our hypothesis will provide a safe and efficacious material for the production of bone leading to reliable fracture healing, circumventing the need for bone grafts, or for direct administration of cells, viruses, or other materials that could lead to significant adverse reactions.

Body: The central hypothesis of this application is that rapid bone formation can be successfully achieved with only minimally invasive percutaneous techniques and without a scaffold, by using cells transduced with adenovirus vectors to express an osteoinductive factor (BMP2), which have been encapsulated in hydrogel material and later photopolymerized at the desired site.

Task 1: To produce high levels of BMP2 from human mesenchymal stem cells transduced Ad5F35BMP2 adenovirus in the presence of tetracycline carrying a red luciferase reporter gene.

a. *To determine if sustained expression of BMP2 is more efficient at inducing rapid bone formation than a pulse of expression using the tetracycline regulated vectors.* ***(Months 0-12)***

These experiments are in progress. We have currently constructed several Adenoviruses that will aid us in completion of these experiments. First we have produced an AdE1BMP2-E3 dsRed virus that will express both dsRED and BMP2 from the same virus, but as totally different transgenes. This allows us to track cells that are expressing BMP2 and determine their viability by the live animal imaging of the dsRED (see section c). Also in this task we proposed to construct and test an adenovirus vector that was able to be regulated by tetracycline, so that we may be able to compare sustained expression to rapid pulsing of BMP2 and determine which if either produced more robust bone formation. Therefore we have constructed an adenovirus that possesses both the tetracycline activator (Tat) and the promoter regulatory element (Tre) on the same virus (Figure 1). With both tetracycline elements on the same vector, we will insure that the essential *trans* activator protein is getting into the same cell as the vector and can therefore repress or activate the transgene by tetracycline. Thus the tetracycline can effectively control all the BMP2 expression versus a subset of cells that had received both elements.

The first set contains the full length human BMP2 cDNA under the control of a tetracycline regulatory promoter element (TRE). As can be seen in figure 1, in the absence of tetracycline the BMP2 expression is turned off. As can be seen in figures 1A and B, we have two versions of this plasmid, one which has a deletion in E3 and one which has the dsRed gene expression cassette. In figure 1 we show the tet on vector, in which the BMP2 is turned on in the presences of tetracycline. We also have constructed the tet off system in which tet represses the expression of the BMP2 transgene.

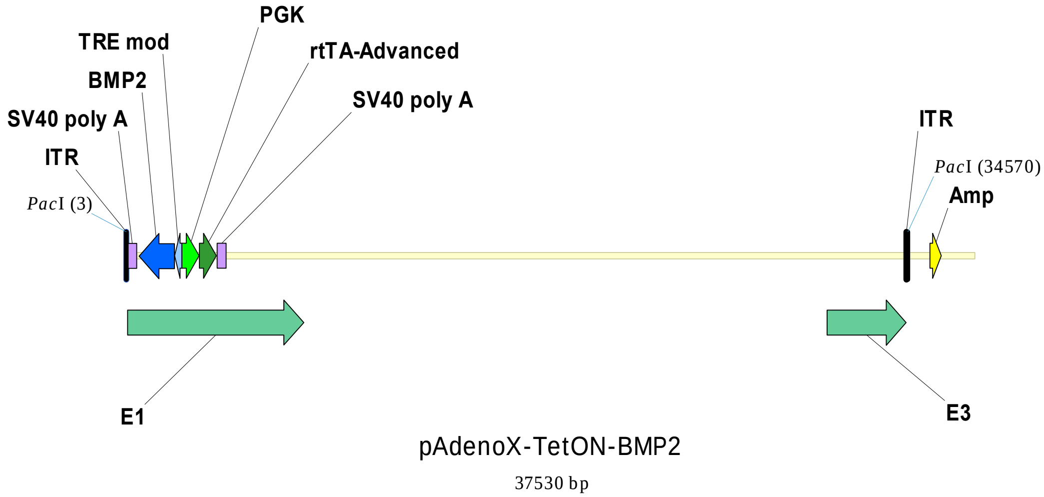

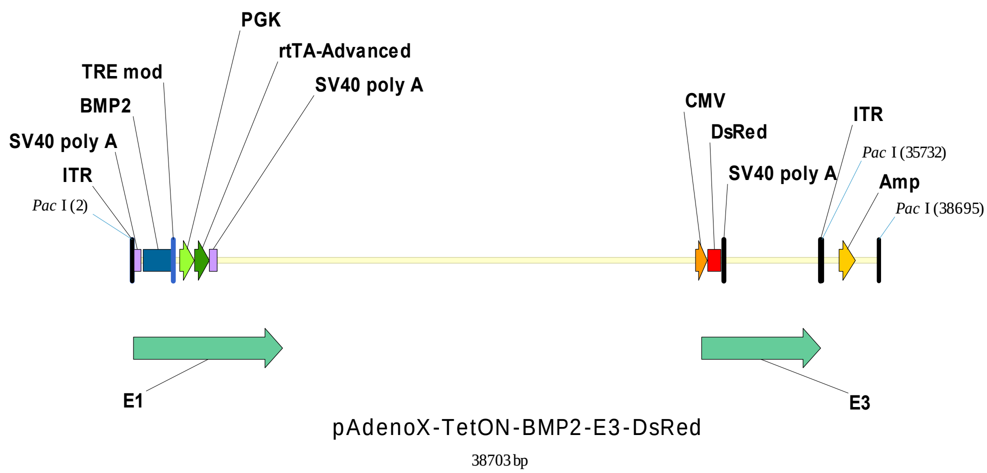

Figure 1: Schematic of the adenovirus containing the both the tetracycline regulatory element TRE and the tet activator protein rtTAT. As can be seen these elements are contained in the E1 deleted region of the adenovirus to control BMP2 expression. The second construct also has a dsRED expression cassette to track the cells expressing the BMP2 *in vivo*. The dsRED is not under tetracycline regulation, but will allow us in the absence of tetracycline to determine the efficiency of transduction, since in this case we expect to obtain little to no BMP2 production. Note we have put the two tet activator and BMP2 gene in opposite directions to avoid promoter interference. Further, we have introduced a PGK promoter driving the transactivator to avoid homologous recombination between the two promoter systems. We are the first to have success placing everything in one virus, and are disclosing this for patenting.

Figure 2 shows results using an AdGFP virus made using this similar tetracycline regulatory backbone. In this experiment A549 cells were transduced with Adtet-GFP in the absence (A) and presence (B) of tetracycline in the media.

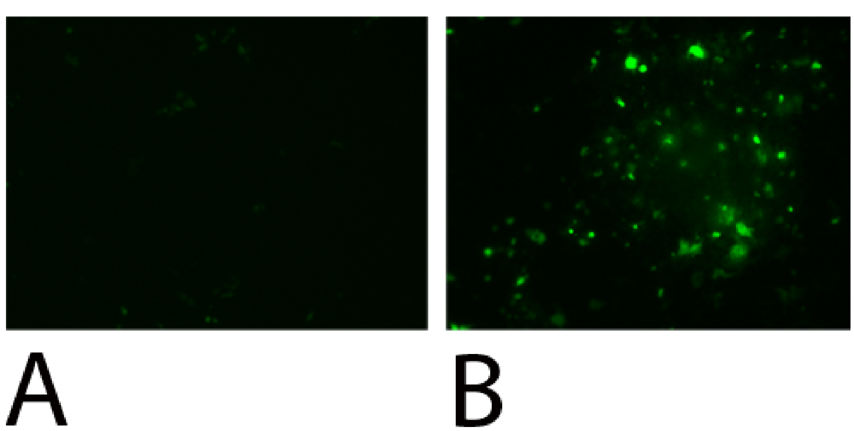

Figure 2: Fluorescent microscopy of A549 cells which have been transduced with Ad5tet-GFP in the absence (A) and presence (B) of tetracycline.

As expected approximately 90% of the cells expressed GFP in the presence of tetracycline while only about 1% expressed the GFP in the absence. This

demonstrates that the regulatory element is capable of substantial attenuation of the transgene expression and will allow us the versatility to look at pulsing BMP2 secretion versus sustained expression, to determine if there is an optimal timing for its production.

However, to implement these vectors for live animal imaging (See section C), both the BMP2 cDNA and dsRED must be under the control of tetracycline. Therefore we are also constructing these to possess a BMP2 IRES dsRED cassette. Although the internal ribosomal entry site (IRES) cassette significantly reduces the reporter gene expression level and thus allows for less sensitive imaging, two TREs elements within the same vector leads to recombination and silencing of one of the genes, making this impractical. Thus the introduction of an IRES is the only method that will allow the dsRED to directly reflect the BMP2 expression and provide feedback as to the sustained versus pulsing of BMP2 in live animal imaging (Figure 3). However we do plan to compare to static results on bone formation obtained by using the first set of vectors described in figure 1.

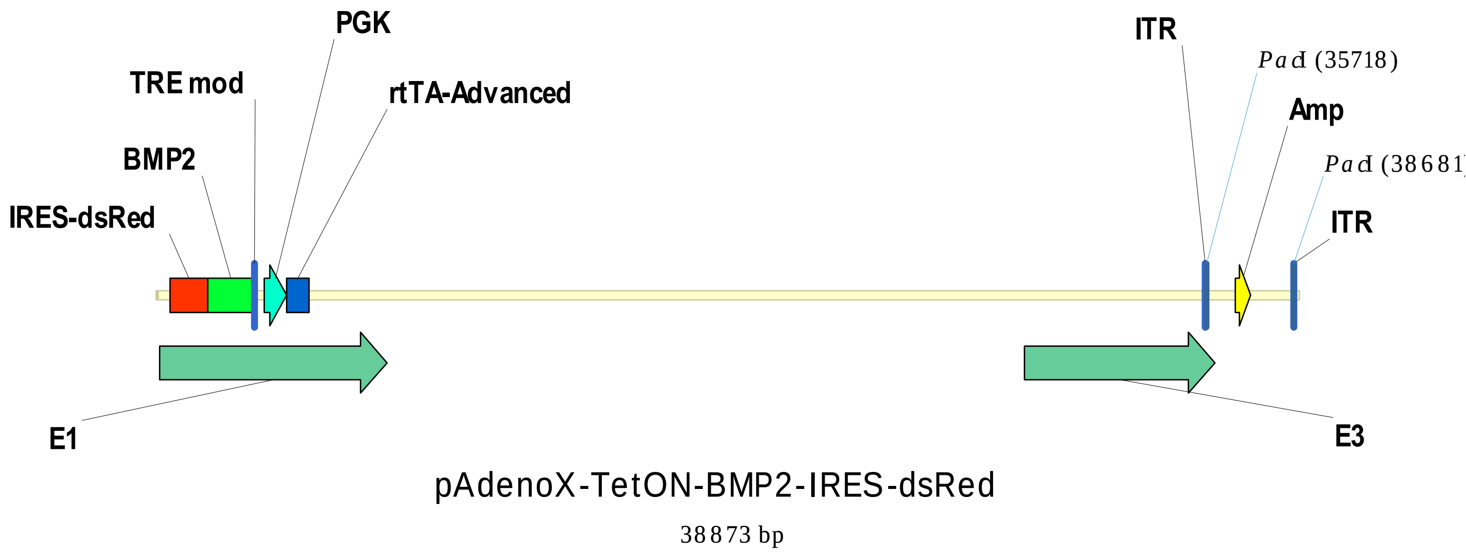

Figure 3: Schematic of a replication defective adenovirus in which the E1 region possesses the Tat expression cassette under a constitutive promoter and a cDNA for BMP2 linked with and internal ribosome entry site (IRES) to a reporter gene dsRED. Thus BMP2 and dsRED will be a single transcript that is then translated into two separate proteins. This transcript will be regulated by tetracycling so that both genes will be regulated.

b. *To determine if longer expression times of BMP2 from cells embedded in hydrogel and longer cellular viability lead to more rapid bone formation than the rapid but short burst of BMP2 release obtained from the cells directly injected.* ***(Months 9-12)***

We are highly focused on completing this aim, using the vectors described in aim 1. We have observed a repressed effect of our cell based gene therapy system on bone formation with inclusion of a carrier as compared to in its absence. We have previously found that our BMP2 delivery cells are rapidly cleared (Fouletier-Dilling *et al* 2007) in the absence of a carrier, whereas inclusion of the cells in a collagen carrier (Gugala *et al,* 2007) or encapsulation of hydrogel (Bikram et al, 2007) greatly reduces the amount of BMP2 secreted to the local environmentand ultimately bone. Interestingly, our preliminary data suggests that inclusion of a carrier such as hydrogel does however, length the lifespan of the transduced cell within the tissues resulting in prolonged BMP2 expression, even though overall it is at a reduced level.

One possible reason for the increase in bone with a pulse may be the role of BMP2 as a morphogen in physiology. That a large pulse allows for a gradient to be established, whereas a longer lesser expression level, may lead to more of a steady state phenomena within the tissues. This may be important for the ability of BMP2 to direct the differentiation of progenitors towards a variety of fates. Perhaps it is as critical to cell fate determination to turn off BMP as it is to have induced it originally. We recently have found the appearance of a novel stem cell population within the peripheral nerves that appears to migrate from the nerve within 24 hours of induction of this assay. These peripheral nerve sheath cells appear to express many factors of the brown adipocytes, yet they also express factors such as osterix, an osteoblast master regulatory factor. This result has led us to question whether the large pulse of BMP2 is capable of setting early heterotopic bone formation in motion, but that the BMP2 must be turned off as in embryogenesis to allow for further advancement of this

process. We know that BMP2 is involved in early neural ectoderm organization and development, and addition of BMP2 to human ES cells leads to neuronal differentiation. We propose that in our model, these early nerve stem cells are an essential component for establishing the necessary environment for stem cell recruitment and differentiation, and that sustained delivery may dampen these processes, but enforcing only an osteogenic pathway, at the expense of other cells types such as vasculature, lymphatics and adipose all essential to the rapid production of bone. Further we hypothesize that the reduced release of BMP2 by inclusion of a carrier may not effectively launch these early stages of heterotopic bone formation, effectively reducing the overall process. We thus are planning to continue these experiments in the next 6 months and complete this work, since it may have a large impact on the final design of our tentative system, as well as explain a large number of reports that suggest recombinant BMP2 products used exclusively in conjunction with a carrier do not work reproducibly.

c. *To demonstrate the termination of BMP2 expression using an Ad5F35tet-BMP2-IRESCBRLuc vector in which expression can be tracked through live animal imaging.* ***(Months 12-24)***

We have currently constructed the Ad5E1BMP2 E3dsRED vector for initial testing. We have found that this reporter to be the most sensitive, and easiest for use in the hydrogel material. We have thus initiated the experiments to track the injected cells and compare the temporal and spatial expression of dsRed *in vivo*, to that obtained from cells in the hydrogel material as described in Aim 1. One anticipated problem was the ability to see the material through the muscle tissues. Further the hydrogel may in fact shield the dsRED signal to some extent. Therefore in the initial experiment we went ahead and started with a single cell number of 5 x 10^6 cells either encapsulated in hydrogel, or directly injected into the muscles. In these experiments human MRC-5 cells were transduced with the Ad5E1BMP2E3dsRED and then either encapsulated in hydrogel, injected and photopolymerized in place, or directly injected into the hind quadriceps muscle. Due to difficulties with the animal facilities, we did not follow the same mice throughout but rather had different mice per time point. However, we are currently set up to do a second study in which we will follow the same animal for a longer period of time.

As can be seen in figure 4, the DSred expression in the cells was readily detectable in all animals. In all cases we used both hind limbs, however, as can been seen in figure 4, often the signal could often only be detected in either the dorsal or ventral view rather than both. As is the case in animal 1, both legs have robust signal only in the two different views, whereas in animal 2 the signal is only detected in the ventral view in both legs. Interestingly, we did not see much back ground signal from the hydrogel material, in fact the signal seemed to be somewhat shielded as expected, however, still detectable in each limb (as marked by the arrows).

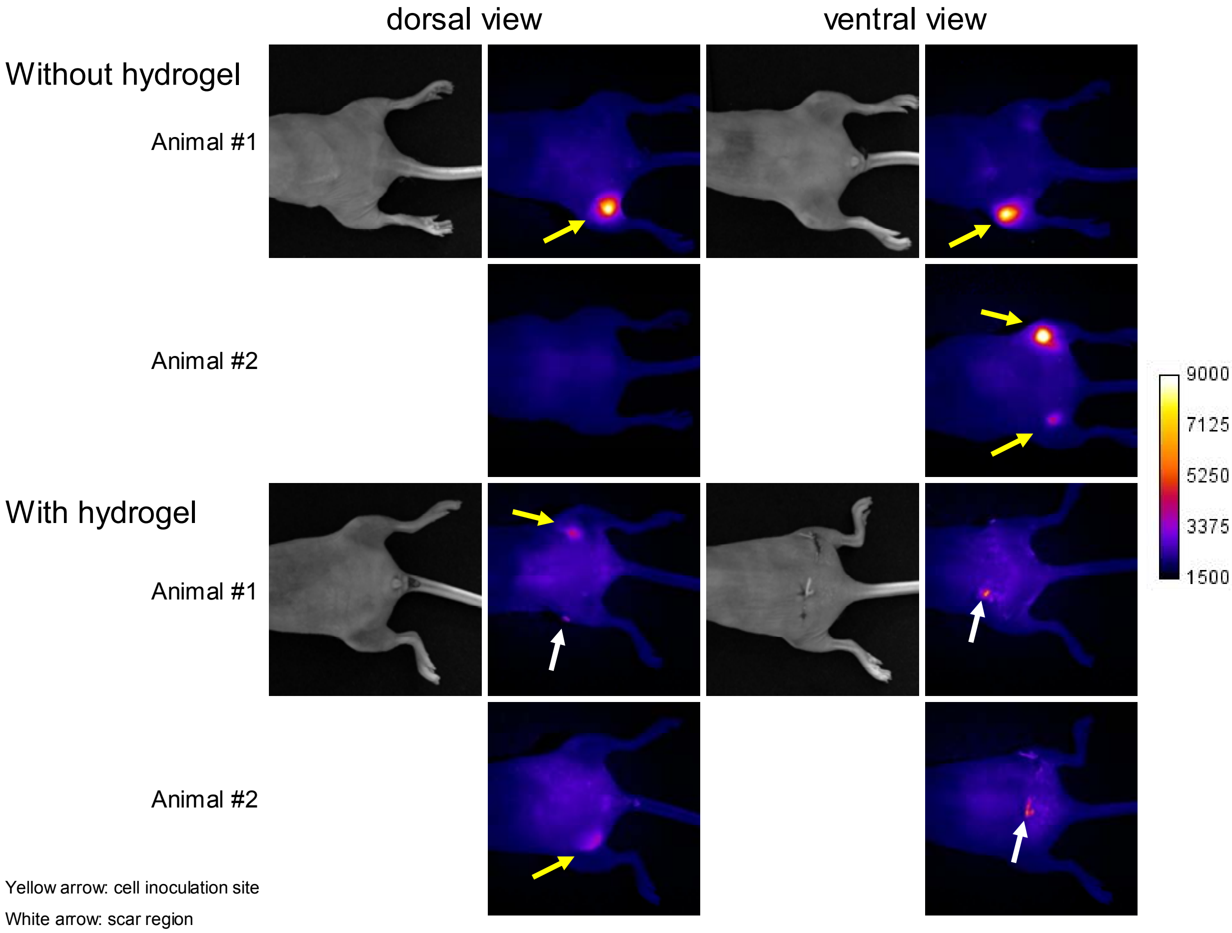

Figure 4: Live animal optical imaging of nude mice which received 5 x 10^6 MRC5 cells transduced with Ad5BMP2 and encapsulated or unencapsulated in hydrogel. In these experiments the cells were directly injected into the quardriceps muscle or fibers were separted, the hydrogel and cells injected, and then the fiberoptic light shown on the gel material to crosslink the material in place. The mice were then imaged 4 days later.

We then imaged mice at a second time point, approximately 7 days after delivery of either the Ad5BMP2 transduced MRC5 cells or those encapsulated in hydrogel. As can be seen in figure 6, we still observe some signal in one of the animals that received the direct injection although it is reduced from that obtained in the animals measured on day 4. However, the second animal directly injected had no signal in either view, suggesting that the DSRed containing cells were no longer present or viable to produce the transgene. This is consistent with our previous work demonstrating clearance of the cells by 7 days. It is intriguing to note why so much signal persists in one limb of animal 1, and we will section the tissues to determine if this is due in part to the stability of DSRed and perhaps was released when the cells were degraded or whether the cells are still present within the tissue. As expected the hydrogel encapsulated cells all yielded detectable signal and consistent in range with that observed on day 4 suggesting that the biomaterial is not only retaining the cells, but capable of prolonging the expression of the transgene.

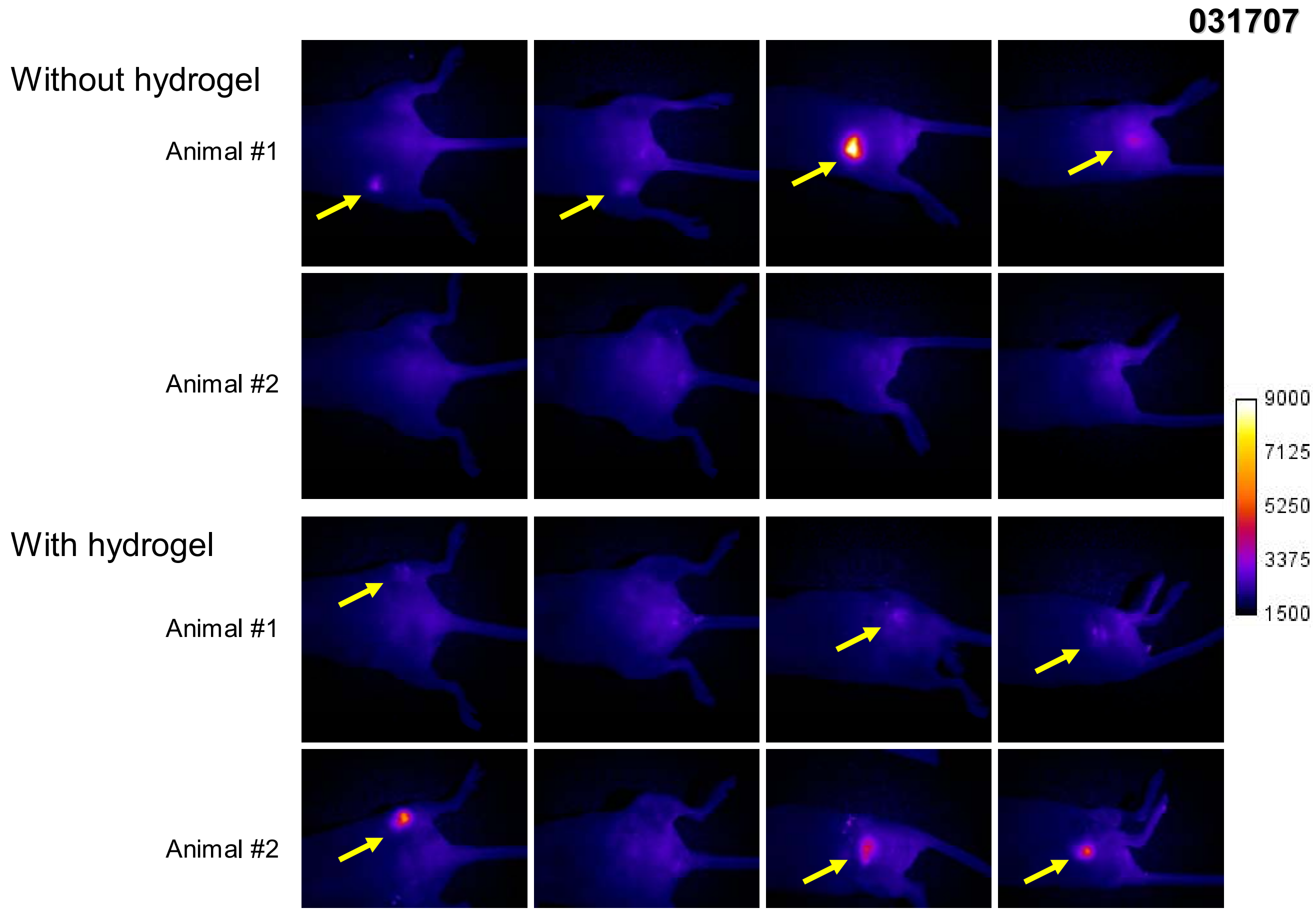

Figure 5: Live animal optical imaging of nude mice which received 5 x 10^6 MRC5 cells transduced with Ad5BMP2 and encapsulated or unencapsulated in hydrogel. In these experiments the cells were directly injected into the quardriceps muscle or fibers were separted, the hydrogel and cells injected, and then the fiberoptic light shown on the gel material to crosslink the material in place. The mice were then imaged 7 days later.

We will next repeat these experiments with titration of the transduced cell number to determine the lower limits of our detection. We will include more time points to determine the length of time the hydrogel encapsulated cells are actually viable in the animals, as compared to the directly injected cells. These experiments are ongoing, and as more vectors are produced will be completed within this next year.

d. *To track BMP2 expression in vivo by identifying cells undergoing BMP2 signaling through confocal imaging which follows the translocation of a Smad 1 to the nucleus.* ***(Months 24-48)***

We initiated these experiments earlier than proposed since the set up of imaging this *in vivo* model is a large undertaking and will require a significant amount of time to validate. Initial experiments have been done to compare and pinpoint the changes in phosphoSmad signaling in tissues receiving the Ad5BMP2 transduced cells, as compared to those receiving cells transduced with control virus. This analysis was done in tissue sections to provide preliminary data before setting up the *in vivo* imaging.

These preliminary experiments will allow us to not only pinpoint locations within the tissues to focus, but also provide us with a time frame of signaling, thus providing incite for the in vivo studies. Figure 6, shows immunohistochemical staining for phosphoSmad using an antibody specific to the active phosphorylated form in tissue sections taken from tissues isolated four days after injection of the transduced cells. These initial experiments were done in wild type (C57BL/6) mice. The phoshpoSmad mice are currently constructed and are being breed to expand there numbers, as well as further characterized as to their exact phenotype.

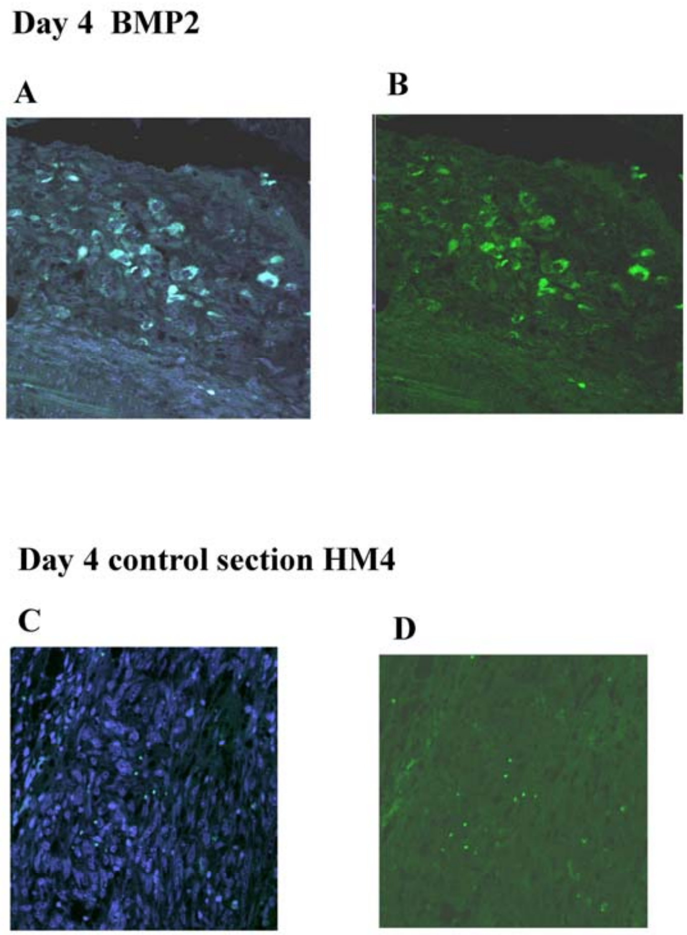

Figure 6: Immnuno-fluorescence staining on tissues isolated four days after receiving Ad5F35BMP2 transduced cells (A and B) or cells transduced with a control virus Ad4F35HM4 (C and D). Sections B and D are stained with Phospho-Smad1/5/8 antibody (1/100 dilution, Cell Signaling technology) and a secondary antibody anti-rabbit Alexa Fluor 488 conjugated. Sections A and C and stained with Phospho-Smad1/5/8 and counterstained with DAPI

We next constructed a BMP signal activation indicator system for use *in vitro* and *in vivo*. We made a targeting construct to modify the Smad1 genomic locus to express the CFP:Smad1 fusion protein at endogenous levels within cells that normally express Smad1. This construct is designed to insert CFP at the N-terminal end of Smad1 by replacing the start codon in exon 2 (Figure 7). This report was tested in transient transfection experiments with COS and HeLa cells, and found to function similarly to the normal endogenous Smad1 protein, and the addition of the CFP reporter did not appear to inhibit it from translocating to the nucleus and activating gene transcription. Using homologous recombination to generate correctly targeted ES cell lines, we have generated three independent ES clones which have been injected into blastocysts for the production of chimera mice. From these chimera mice, we have now obtained germline transmission in the animals and we are currently characterizing them for the expression of CFP. Therefore these mice will be available for testing in the next 6 months, and these experiments should be partially completed in this upcoming year.

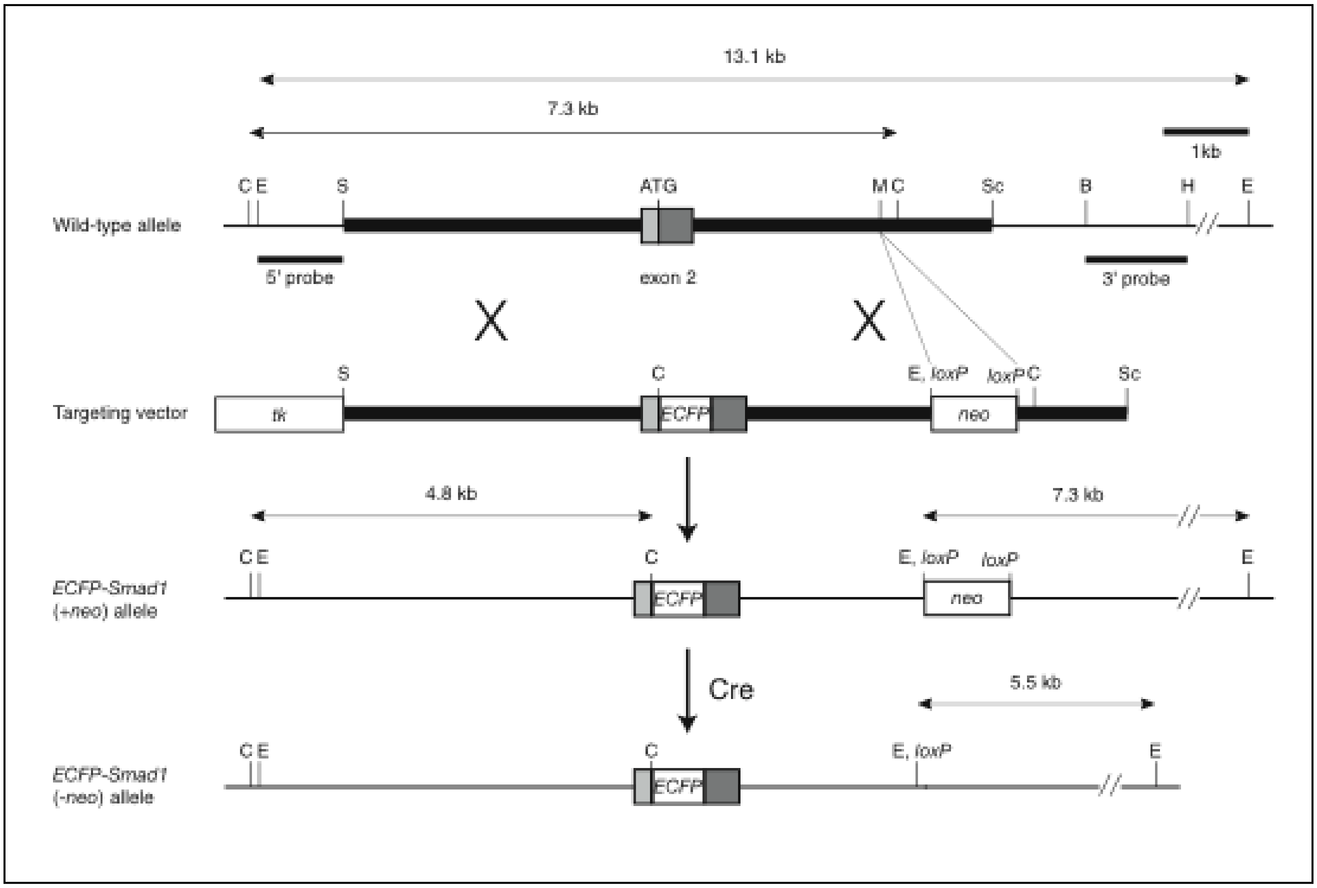

Fig. 7. *ECFP-Smad1* targeting strategy. Partial map of the mouse *Smad1* locus (top), showing the region containing exon 2 that encodes the ATG translation start site. The targeting vector is designed to create an ECFP-Smad1 fusion protein. A floxed neo expression cassette was added at an *Mlu*I (M) site in intron 2 that brings in an additional *Eco*RI (E) site. Targeted ES cell clones are identified by Southern analysis by digestion with *Cla*I (C) and hybridization using a 5' external probe and *Eco*RI digestion and a 3' external probe. The sizes of wild-type and targeted DNA fragments are indicated. Cre recombinase is used to remove the neo cassette. Thick line, region of targeting vector homology; light shaded boxes, 5'untranslated region; dark shaded boxes, *Smad1* coding region; B, *Bam*HI; H, *Hind*III; S, *Sal*I; Sc, *Sca*I; tk, HSV thymidine kinase expression cassette.

e. *Approximately 470 mice will be used in the experiments in this task. NOD\Scid 36 mice/experiment and we request three experiments, plus additional for breeding or 250 total and SMAD 1= 63 mice/experiment and we request three experiments, plus several for breeding or 220 total.*

Task 2: To design an optimal hydrogel material that will rapidly promote endochondral bone formation and be capable of removal through bone remodeling processes.

a. *Optimize and develop a hydrogel that can be specifically degraded by osteoclasts.* ***(Months 0-24)***
We have synthesized the peptide MGPSGPRG (Gowen et a;1999) using a 431A solid-phase peptide synthesizer (Applied Biosystems, Foster City, CA). In order to make degradable PEG, we start with PEG-DA-SMC (succinimidyl carbonate). The PEG-SMC is conjugated with our peptide in order to get PEG-PEPTIDE-PEG. So, we expect to obtain three peaks representing the completely conjugated product: PEG-PEPIDE-PEG, incompletely conjugated product: PEG-PEPTIDE and unconjugated product: PEG-SMC (Figure 8).

Synthesis of Cathepsin K degradable PEGDA hydrogel

- Cathepsin K-sensitive sequence (CTSK):
  - MGPSGPRGK
- Control sequence:
  - MPGSPGGRK
- Conjugate with 3400 Da PEG-SCM

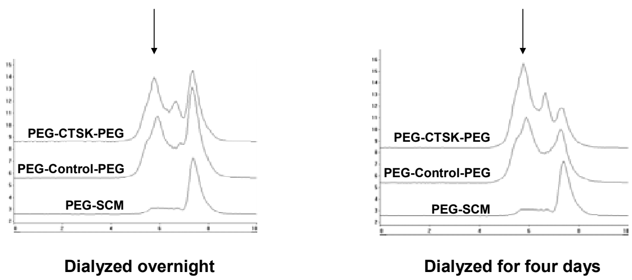

Figure 8: Results of HPLC analysis of the conjugation of peptide with the PEG-DA hydrogel.

We have run GPC tests on it and the results indicate that there is still unconjugated PEG, ie: we have PEG-Peptide or free PEG in the preparations. We have tried changing the ratio of peptide to PEG, changing the length of conjugation time, increasing the pore size of the dialysis membrane and changing the length we dialyze the conjugation products. These have led to a higher concentration of PEG-PEPTIDE-PEG as indicated by the GPC results (Figure 8). We have cathepsin K (Calbiochem; Cathepsin K, His•Tag®, Human, Recombinant, *E. coli*) and are ready to test their degradability.

The next step in developing this material was to test whether the conjugation of the cathepsin K site is enough to degrade a polymerized peptide. We placed microbeads of the hydrogel in the 25 μL cathepsin K vial (stock solution 0.2 mg/mL cathepsin K) incubated at 37°C. The PEG-peptide-PEG hydrogels (where “peptide” refers to the cathepsin K degradable peptide) were tested for swelling and degradation in PBS and cathepsin K, respectively (n=1). A swelling hydrogel typically has a logarithmic curve, like the PBS curve, where the weight of the gel increases and reaches a maximum. A degrading hydrogel will initially show an increase in weight as broken bonds allow more water in, allowing the hydrogel to swell more. Then the swollen weight will drop dramatically. Figure 9A and B shows evidence that the hydrogels are at least partly degradable. However, the results also suggest that the material cannot be completely degraded suggesting the PEG-Peptide-PEG is limiting, or that the sites are not efficiently digested. To circumvent the latter, we are resynthesizing the peptide to include additional 3 glycines on either end to lengthen the protein region and ensure that cathepsin K can reach it efficiently within its PEG backbone.

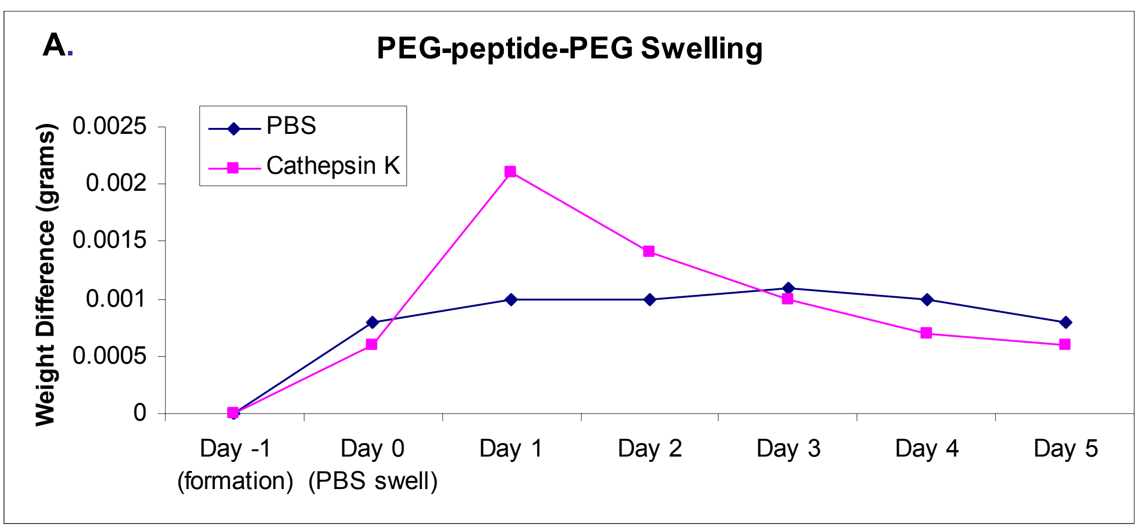

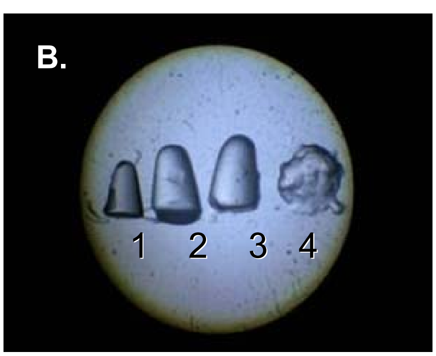

Figure 9: Swelling test of the Cathepsin K degradable peptide. **A.** Weight changes upon swelling during degradation. **B.** Hydrogels after swelling and degradation. (1) PEG-CTSK-PEG in buffer w/o proteinase K; (2) PEG-CTSK-PEG w/ 0.125 mg/ml; (3) PEG-control-PEG w/ 0.125 mg/ml; (4) PEG-CTSK-PEG w/ 0.250 mg/ml after compression.

Hopefully with the additional amino acids on the peptide site, any constraints the protease may have in binding for digestion of the site will be alleviated.

We have been recently testing the new protease site which now has a glycine repeat sequence was designed into the peptide in order to act as a spacer. Thus the modified peptide sequence is GGGMGPSGPWGGK, see figure 10. The W is tryptophan that we will

use to track the degradation of the hydrogel by measuring tryptophan release into the media by taking Ultra-Violet/Visible (UV/VIS) Spectrophotometry absorbance measurements at 280 nm.

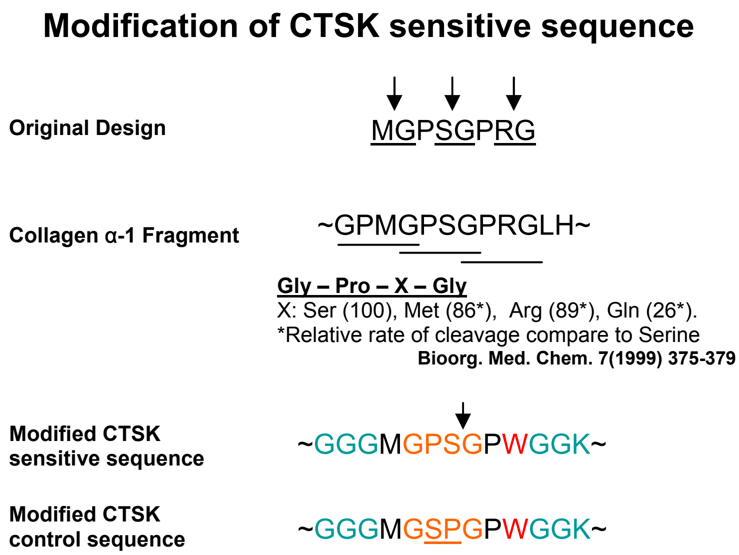

Figure 10: Schematic of the changes made in the peptide to introduce the cathepsin K protease site into the PEG-DA hydrogel.

Rather than incorporate this new peptide immediately into a PEG backbone, it was tested directly. We ran mass spectrometry on the peptide in order to see if the predicted molecular weight (1143.43) of the peptide was present. We found a peak at 1143.9, indicating success of the peptide synthesis. Next, we incorporated the peptide with activated cathepsin K and repeated the mass spectrometry. The 1143.9 peak was now absent, and present were predicted cleavage products (figure 11)

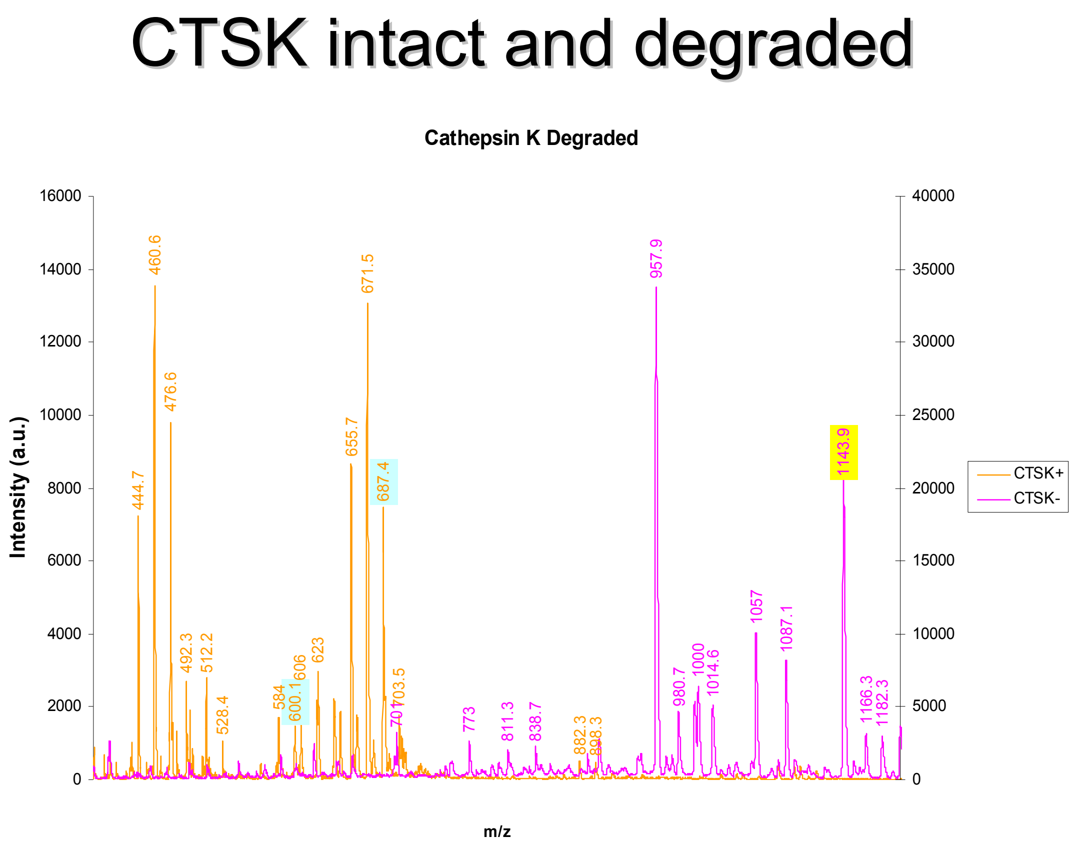

Figure 11: Mass spectrometry of the peptide consisting of the cathepsin K protease site (CTSK) before and after cleavage with the protease.

We also discovered that our control peptide had a cleavage site that we did not immediately notice until after it had been made. We will need to re-prepare the control to eliminate this site.

We proceeded with degradation tests when prepared hydrogels degraded almost immediately in proteinase K. To prevent artifact from increased enzyme concentration due to evaporation over time, we used a concentration of proteinase K that would degrade over hours, rather than days, and matched that concentration for the cathepsin K degradation tests. We were pleased to see that the tryptophan release test suggested that the hydrogels would be completely degraded by the cathepsin K similarly to when protease K was added (figure 12). This demonstrates that they had adequate incorporation of the peptide into the hydrogel and that the selective enzyme cathepsin K could cleave it.

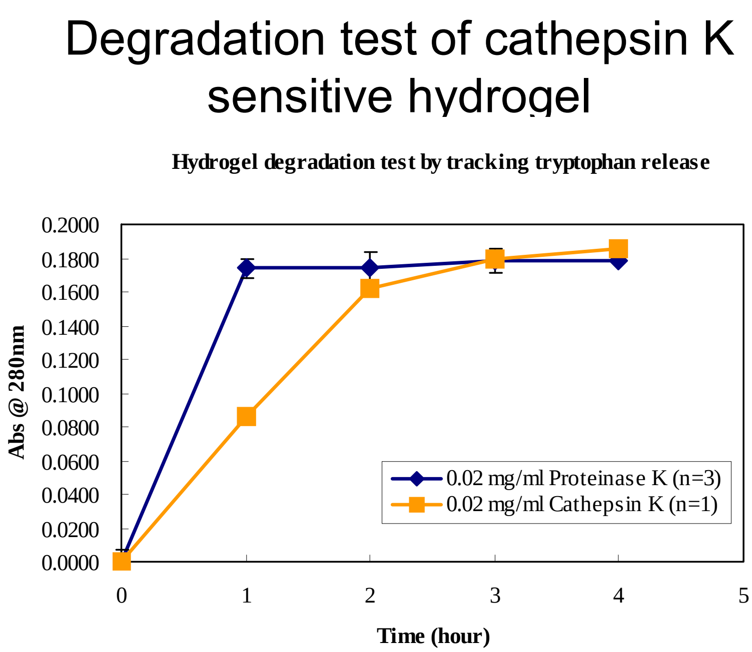

Figure 12: Trytophan release demonstrated complete degradation of the hydrogels by either the proteinase K or cathepsin K.

We next need to demonstrate the selective cleavage using enzymes that do not cleave. These studies have already been initiated. Further, we will also run concentration curves to determine the minimum amount of cathepsin K required for efficient degradation. Figure 13 shows the degradation of the hydrogel in the presence of 0.02 mg/ml and 0.1 mg/ml. As can be seen, 0.1 mg/ml can completely degrade the hydrogel similarly to more non-specific 0.2 mg/ml collagenase. Figure 13 also demonstrates the stability of the conjugated hydrogel in hanks buffered saline (HBS) without protease.

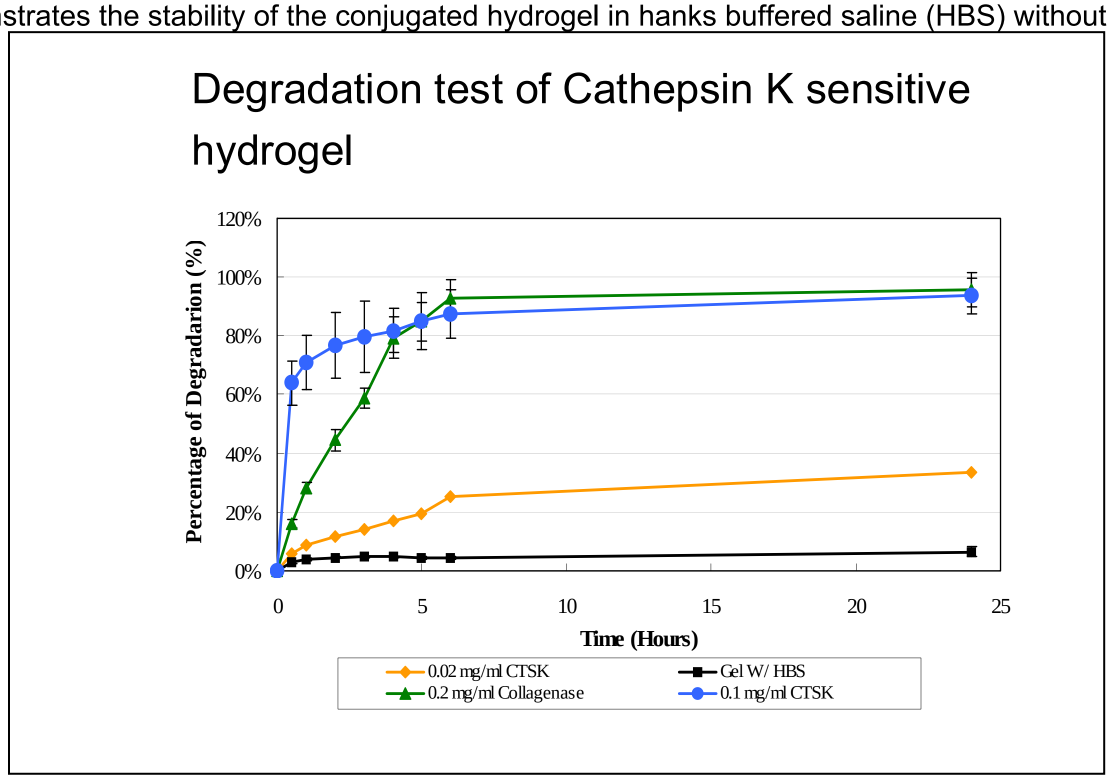

Figure 13: Degradation of hydrogel over time.

b. *Engineer cellular binding sights within the hydrogel to determine if this improves cell viability of the transduced cells, and in turn BMP2 expression, and to tentatively enhance the migration of mesenchmyal stem cells to the sight of bone formation.* ***(Months 0-24)***

We have actually been changing this aim to meet the needs of both the encapsulated cells but also allow for the selective degradation. Since the recruitment of osteoclasts often comes from the expression of RANK ligand (RANKL) and degradation requires RGD binding, we have designed a large number of RGD binging sites within the hydrogel material (Yang et al, 2005). This should greatly enhance binding and long term viability of our encapsulated cells, but it will also permit the hydrogel to be degraded by osteoclasts which adhere to the bone surface through RGD, form a ring structure (Figure15) of the ruffled border (Hollberg *et al*, 2005) and then activate a proton pump as well as secrete specific proteases such as cathepsin K. Therefore, RGD is critical to the recruitment, adherence, and resorption of the hydrogel by osteoclasts. RGDS will also aid in recruitment and binding of other cell types to the surface of the biomaterial, and allow for the newly forming bone to be close enough to the surface that it can easily fill in the areas removed by remodeling.

c. *Test addition of proteins that may enhance the BMP2 bone inductive response, such as VEGF-A or –D and compare enhancement of bone formation.* ***(Months 24-36)***

We have a manuscript coming out that shows significant elevation in these VEGF proteins after expression of BMP2 in the tissues (Appendix). Thus we do not believe that this will add anything to our current system. In the event that minimal BMP2 is made, VEGF seems to emphasize the bone reaction, presumably since it is one of the first downstream proteins we observe elevated after addition of the AdBMP2 transduced cells. However, we are getting significant elevation of these proteins through using our cell based gene therapy system, and thus we find combinations of these do not enhance the bone reaction. Therefore we propose to discontinue this testing.

d. *Test these gels in vitro.* ***(Months 12-36)***

We have previously tested the degradation profile of the cathepsin K (CTSK) sensitive-hydrogel *in vitro* with proteinase K, collagenase, and cathepsin K (Figure 14). Before proceed with the animal study, we first performed a cell based *in vitro* test to demonstrate that the CTSK-sensitive hydrogel can be gradually remodeled by osteoclasts (OCs). We used the RAW264.7 monocyte cell line that has been demonstrated in the literature to undergo fusion and osteoclastogenesis in the presence of 20 ng/ml nuclear factor kB ligand (RANKL). We first differentiated the RAW264.7 cells with 20 ng/ml RANKL in standard tissue culture for 6 days, at which time we observed that multi-nuclei, osteolclast-like cells by the end of the differentiation period. Then 1.5 x 10^5 cells/cm^2 osteoclasts-like cells were seeded on 10% (W/V) hydrogel (100% CTSK-sensitive hydrogel), which contained 10mM acryl-PEG-RGDS and Alexaflour 680 labeled acryl-PEG-RGDS. The differentiated osteoclasts-like cells were then cultured on the hydrogel surface in RANKL-free medium for 24 hours before further analysis. The cells and gel were than fixed and stained with DAPI and rhodamine phalloidin after 24 hours. Images were taken by LSM-5 LIVE and then processed by Image J and OsiriX (Figure 14 and 15).

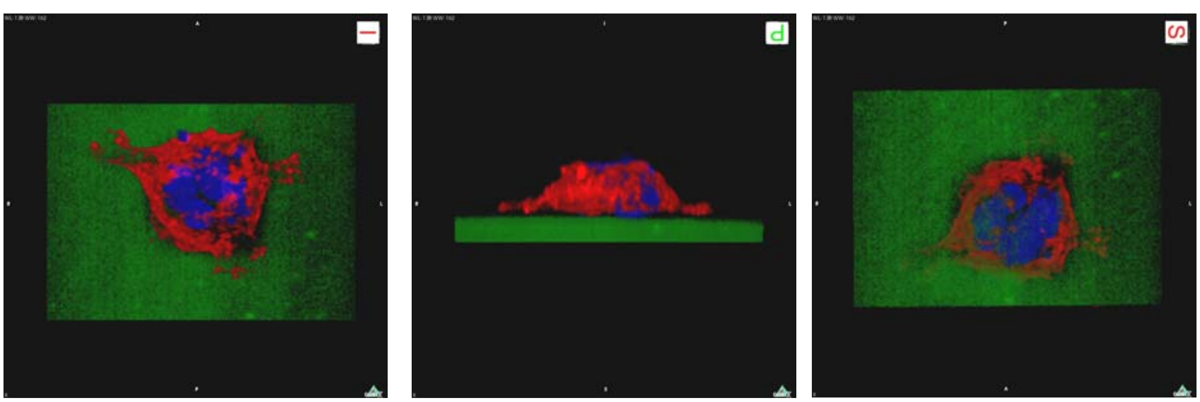

Figure 14: Fluorescence images from the (a) top, (b) side, and (c) bottom view of a single osteoclast on the hydrogel surface. The hydrogel was labeled with Alexafluor 680 fluorophore (green), which is conjugated with the acryl-PEG-RGDS and incorporated into the hydrogel by UV light induced photo-polymerization. The cells were fixed and permeabilized before stained the nuclei and F-actin by DAPI (blue) and rhodamine phalloidin (red) after cultured on the gel for 24 hours. The resorption site is located underneath the osteoclasts, which was shown by a loss of the fluorescent intensity of Alexafluor 680.

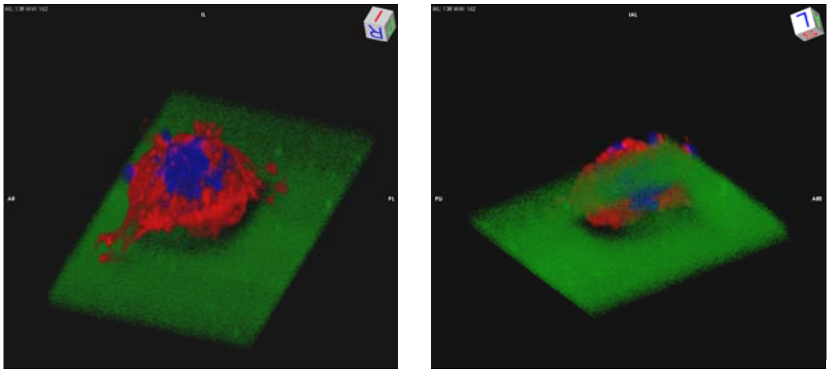

Figure 15: 3D reconstruction images of an osteoclast on the hydrogel surface. The images from the top (a) and bottom (b) view of the hydrogel were generated by Image J and OsiriX. The resorption pit on the hydrogel surface can be clearly observed from different angles.

As shown in Figure 14 and 15, the resorption site is observed underneath the osteoclast, which was shown by a loss of the fluorescent intensity of Alexafluor 680. This demonstrates that the hydrogel is being cleaved by the osteoclasts. Our next set of experiments which is ongoing is to show the inability of general fibroblasts to cleave the hydrogel. We propose to measure the area of degradation with the generalized fibroblasts as compared to the osteoclasts to confirm that we are getting selective degradation. These experiments are expected to be completed within the next 3 months, at which time we plan to publish this work.

d. *Test these gels in vivo.* ***(Months 36-48)***
e. *Approximately 500 mice (NOD\Scid) will be used to complete the experiments in this task. This will provide us with the 468 we need to complete the proposed experiments as well as an additional 32 for breeding stock.*

Task 3: To achieve rapid bone formation by percutaneous injection of the encapsulated Ad5F35BMP2 transduced human bone marrow mesenchymal stem cells (hBM-MSCs) into the adjacent musculature of athymic rats in a model of nonunion.

a. *Obtain approvals through the DOD institutional review board for approval to work with the human mesenchymal stem cells.* ***(Months 0-12)***

We have approval to use human mesenchymal stem cells, and are currently testing these cells for both viability and BMP2 secretion after encapsulation in the PEG-DA hydrogel. Also we have been working on developing the protocols for encapsulation of the rat fibroblasts to confirm maximum BMP2 secretion and viability. We wish to confirm that these two cell types function in the hydrogel similarly to the cells in previously published experiments. These experiments are quick and will be completed soon, thus providing us confirmation that we need to test and compare our systems in the two proposed models.

b. *Once the gels have been modified to offer optimal properties for bone formation and removal, we will test these in a rat model of a critical-size defect. We will demonstrate the ability to induce bone healing in the presence of tetracycline.* ***(Months 24-40)***
c. *Analyze the modified injectable hydrogel for optimal volume, in vivo crosslinking, design, selective degradation, and inflammatory reaction using both live animal imaging and histology.* ***(Months 24-48)***
d. *Bone healing will be tested both biomechanically as well as radiologically using microCT to confirm the fusion.* ***(Months 40-48)***

Approvals have been obtained from Baylor College of Medicine and more recently from the Department of Defense for both the animal experiments and use of the human materials. Because we were able to complete this rapidly, we have initiated the studies using a critical defect rat model. We recently have also been focused on using an alternative to this model, which provides a much faster more reliable critical size defect, for testing of the biomaterials. We have approval for this amendment from the Baylor College of Medicine IACUC committee. In this model, a 4-6 mm defect is cut in the rat fibula, with the adjacent tibia remaining intact and thus provides the necessary stabilization. Thus no additional hardware is required, and the surgical procedure is quite rapid. Fig 16 shows a representative x-ray of the fibula, which received the defect two weeks prior. As seen in the x-ray, the defect has not healed. However, smaller sized defects actually have healed within this same time period. Therefore we believe this is a relevant model for testing of the biomaterials (see next section).

Briefly, this model involves introducing a critical size defect into the rat fibula. Unlike humans, the rat fibula unites with the distal tibia and does not comprise a part of the ankle joint. Recent measurements show the potential to introduce a large enough defect to be critical size. Because the tibia will remain intact, this eliminates the need for rigid fixation with additional hardware. This is much safer for the animals, which will be able to ambulate normally. Thus the surgical times are greatly reduced as well as post-operative stress on the animals.

In this model, the rat fibula will be exposed by dissecting through the plane between the anterior and the superficial posterior muscle compartment to expose the bone. The periosteum surrounding the bone will be lifted during this procedure. Using a ronguer, specific sized deletions of critical distance will be introduced into the bone. Then, either Ad5F35BMP2, Ad5F35Empty cassette transduced cells, or the corresponding PEG-DA hydrogel encapsulated cells will be introduced into the defect site and healing will be monitored at weekly intervals ranging from 1-8 weeks.

In our pilot experiment, we introduced a range of defects into the fibula, and approximately 6 weeks later, euthanized the animals to evaluate bone healing. The results were extremely surprising in that all defects introduced into this bone were unable to heal. Further, the bone appeared to undergo significant resorption (figure 16).

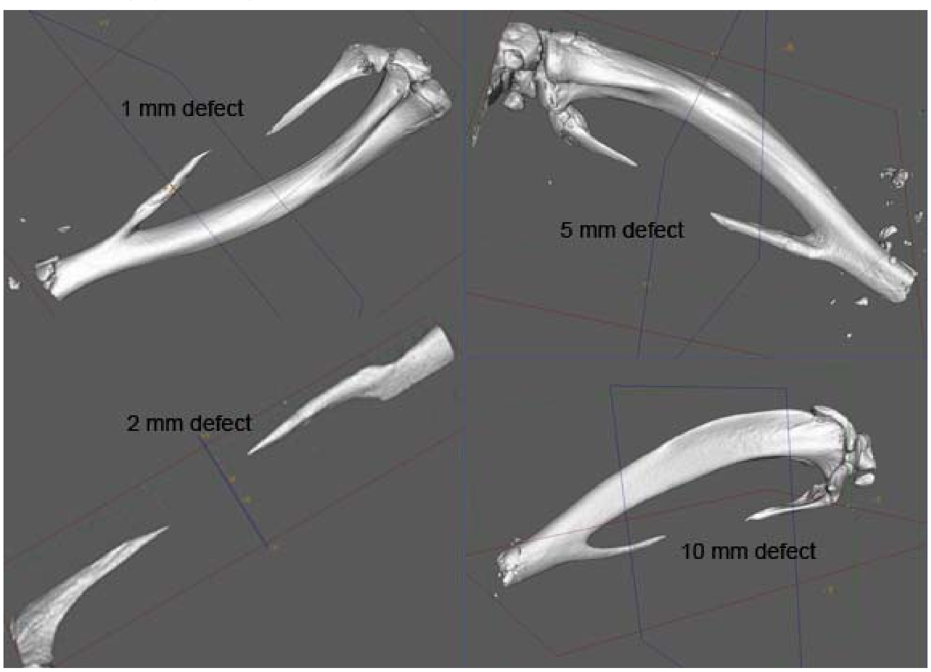

Figure 16: MicroCT analysis of the rat fibula 6 weeks after introduction of varying size defects. The numbers in mm represents the original size defect introduced into each sample. The samples shown are representative of n=3 samples.

MicroCt analysis of the samples revealed bone healing at the boundary of the defect. Samples examined at 2 weeks appeared to have a non-mineralized central core, suggesting that the bone had not formed over the defect boundary, whereas at 6 weeks, the end of the bone appears to be mineralized with no visible central core. As can be seen in figure 16 however, the defects

appear to be substantially larger than the original defect that was introduced and the ends of the nonunion appear to be angled suggestive of substantial bone resorption rather than formation. This may be due in part to the small size of the bone, lack of substantial marrow component, and removal of the periosteum; however, it provides an extremely important model for bone healing. This model is not only reproducible, but thus provides one of the most rigorous models for inducing bone healing. We propose that introduction of the heterotopic bone at this site will not only favor formation of resorption, but will fuse into the skeletal bone to create adequate healing. Further, we propose to look determine the role removal of the periosteum is playing in either the bone resorption or the lack of bone repair.

To determine if the periosteum could be playing a critical role in induction of resorption of this bone, we analyzed histologically the bone sections removed from the long bone. Interestingly, the fragments varied dramatically, with some lacking periosteum, suggesting if was removed during exposure for introduction of the defect; while others actually had both the periosteum as well as muscle tissue suggesting that this is not the reason for the significant resorption (data not shown). Most likely the resorption is stemming from lack of use of the bone, due to the fusion. The bone appears to resorb to a specific length from the tibial fusion site, and then stop which would be consistent with the resorption being associated with the lack of weight bearing load. Based on this finding, the model becomes an extremely relevant and difficult model for testing bone healing.

As a pilot experiment we tested the ability of Ad5BMP2 transudced Wistar rat fibroblasts to heal the critical size defect. Briefly, the bone was exposed, and a 3 mm defect was introduced. Then approximately 5 x 10^6 Wistar rat fibroblast cell line transduced with either Ad5BMP2 or Ad5empty cassette (2500 vp/cell) were injected into the defect and the area closed with suturing. Bone formation and any potential healing was allowed to occur for 4 weeks, and then the animals were euthanized and the limbs analyzed for new bone formation using microCT.

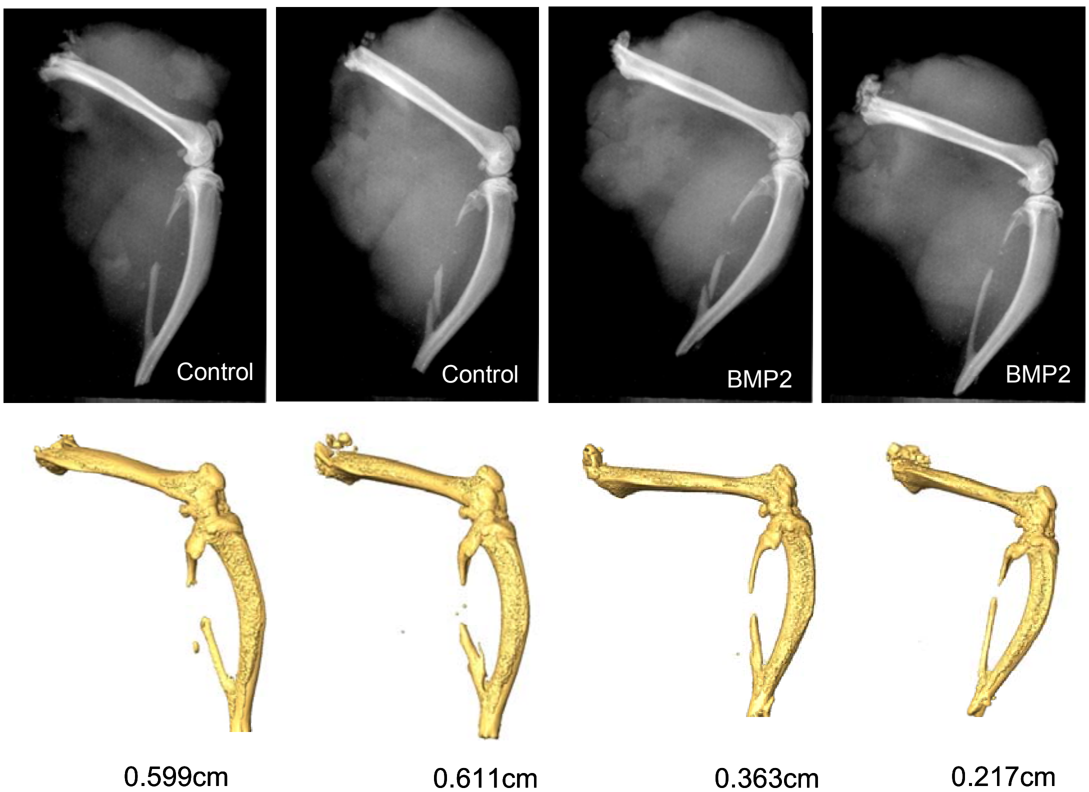

Figure 17: MicroCT of rat fibula 4 weeks after introduction of the critical size defect. In all defects, we introduced a matched rat fibroblast cell line transduced with (2500 Vp/cell) in the presence of a polyamine of either Ad5BMP2 or Ad5empty cassette control virus. The transduced cells were resuspended in PBS and then injected into critical size defect void.

As seen in figure 17, the results demonstrated that we did not get complete healing with obvious well mineralized tissues in this time frame; however, we did observe some new bone formation, as well as blocked the resorption in the remaining fibula. This was consistent for the BMP2 group whereas the groups receiving the control cells showed an enhancement in the size of the defect, stemming from the resorption. As measured by the microCT, the defect in one of the BMP2 samples appeared to be 0-1 mm less

than the initial defect introduced, suggesting again new bone formation whereas the controls were approximately 3-4 mm larger than the original defect (Figure 17). We are currently analyzing these tissues histologically to determine the extent of the new bone formation and its location, whether orthotopic or heterotopic. Further we are analyzing and quantifying the BMP2 expression from the transduced rat fibroblasts to determine the transduction efficiency.

We need to confirm that our current transduction methods are leading to adequate secretion of the BMP2. To determine the transduction efficiency we measured BMP2 release into the culture supernatant by ELISA (R& D systems). Briefly, two different rat cell lines; ARIP which is a buffalo rat cell line and BRL3A which is a wistar rat cell line, that was used the previous experiment (figure 18). We also included Ad5F35BMP2 transduced MRC5 cells, which routinely has 90% or higher transduction efficiency and BMP2 secretion. The rat cell lines were transduced with Ad5BMP2 or Adempty, the negative control virus, at various MOI (2500 or 5000 virus particles (vp)/cell. Figure 20 shows the amount of BMP2 in an equivalent volume (100 ul) of tissue culture media collected 72 hours after transduction. A standard curve using recombinant BMP2 protein was included for quantification.

As can be seen in figure 18, the cell line ARIP at the highest adenovirus dose secreted roughly the same amount of BMP2 as the positive control cell line MRC5. However, interestingly, the second rat cell line BRL3A which was used for the *in vivo* experiment produced a significant amount of BMP2 as well. Therefore the lack of healing and more visible bone formation in the defect site in our rat model, may reflect additional problems such as a rejection to the cell line, since rats are not as inbred and genetically defined as the laboratory mouse populations. We are currently analyzing the histology from these experiments as well as generating a skin fibroblast cell line from the rats themselves.

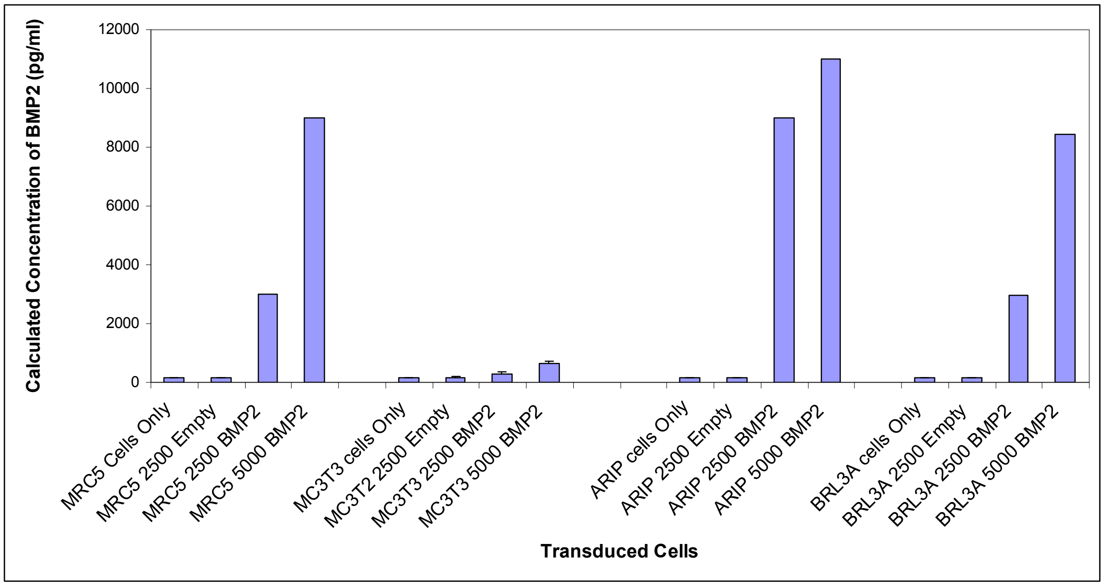

Figure 18: Quantification of BMP2 protein in culture supernatant 72 hours after transduction of the cells with AdBMP2. BMP2 protein was quantified by ELISA

We next tested our system by injecting Ad5F35BMP2 transduced MRC5 cells which efficiently take up the adenovirus and secret BMP2, into a critical size defect in an athymic rats (n=3). The rats were then euthanized 6 weeks later and the limbs x-rayed to detect the new bone. Figure 18 and 19 show representative images of defects which received the BMP2 transduced cells. Figure 18 shows the bone healing approximately two weeks after injection of the BMP2 transduced cells. As can be seen in the figure (arrow) the heterotopic bone appears to be more adjacent to the defect site which may have attributed to the lack of filing the defect completely. In figure 19, 6 weeks after the induction of bone formation with BMP2 we see significant amount of bone in the lower panel in the defect area with almost complete healing, while the control (top) has resorbed. Two potential possibilities exist, first the lack of any fixation of the bone ends, may have led to enough

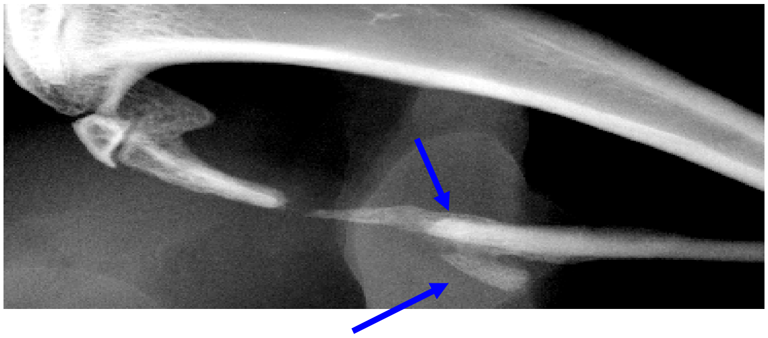

Figure 19: Bone formation in a critical size defect, by induction of heterotopic ossification using a cell based gene therapy system.

movement to introduce a joint space rather than complete healing. Alternatively, we injected the transduced cells into the muscle adjacent to the end of the defect. With injecting a single site, we potentially localized the heterotopic ossification to one side, and hindered bridging of the bone defect. We hypothesize that with the addition of the hydrogel materials we may be able to better target the bone formation to the entire defect site. However, we must first complete our optimization reactions as described in Task 2.

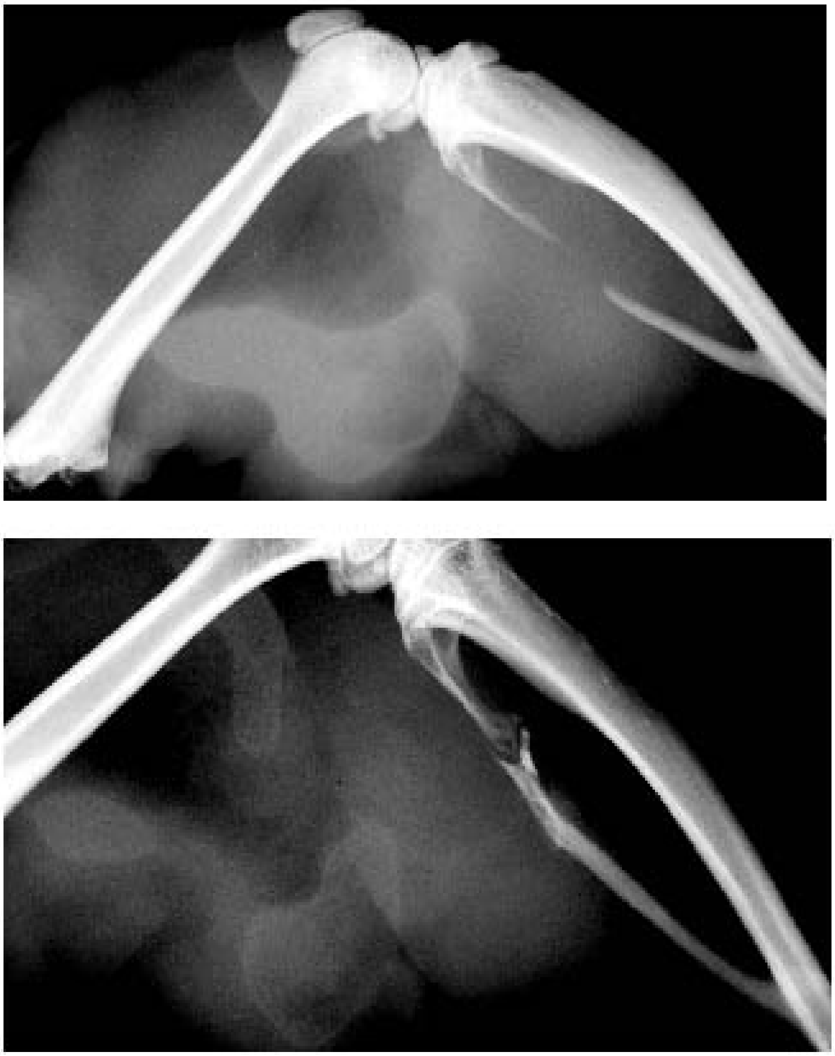

Figure 19: Critical size defect was introduced into the fibula of athymic rats. The top panel, shows the resultant defect after cells transduced with the control vector were introduced directly into the defect. Bottom panel shows the resultant bone formation within the critical size defect after cells transduced with AdBMP2 were introduced. Rats were euthanized approximately 6 weeks after introduction of the cells.

e. *Approximately 230 rats total. We request 120 NIH nude athymic rats for experiments and 108 Wistar rats to complete the experiments in this task.*

Key Research Accomplishments:

Task 1: To produce high levels of BMP2 from human mesenchymal stem cells transduced Ad5F35BMP2 adenovirus in the presence of tetracycline carrying a red luciferase reporter gene.

- We have determined that DSRed is the most sensitive of the reporter modalities for detecting the cells in the hydrogel material after introduction into the mouse muscle.
- We have preliminary experiments that suggest that the hydrogel is capable of expanding viability and transgene expression. However, the lifespan is not expanded as greatly as expected, therefore, we are further optimizing the hyrdogel to improve cell health within the biomaterial.
- We have constructed several adenoviral vectors that have a reporter gene, the BMP2 transgene under the regulation of a tetracycline regulatory element (TRE), and the tetracycline trans activator protein expressed from the same vector. We are currently working on completing the construction of a adenovirus vector that will express the BMP2 and DSRed from a single transcript which is regulated by tetracycline. Once completed will continue to determine if rapid pulsing of BMP2 is more optimal for robust bone formation than sustained expression.

Task 2: To design an optimal hydrogel material that will rapidly promote endochondral bone formation and be capable of removal through bone remodeling processes.

- We have constructed the cathespin K protease site, and introduced it into the hydrogel material.
- We have initially tested this material and found it to be selectively degraded by cathespin K as compared to other proteases.
- We have shown that osteoclasts will adhere, form ruffled borders, and start to resorb the material, presumably by the production of cathespin K.
- We have introduced RGD peptide binding sites to the hydrogel material to provide adhesion for the osteoclasts, as well as to extend the life span of the cells within the gel.
- We have engineered RANK ligand into the hydrogel material which can be bound by the osteoclast precursors to induce osteoclastogenesis, similar to skeletal remodeling. In normal bone remodeling RANKL is released by the osteoblasts to induced osteoclast differentiation, and resorption. Thus it will aid in allowing the biomaterial to function similar to normal bone matrix.
- We are finishing these *in vitro* experiments by demonstrating the inability of other fibroblasts to degrade the material. We have preliminary data that we are currently quantifying to demonstrate the amount of hydrogel degradation we observe in the presence of osteoclasts versus other fibroblast cells, which may adhere in the *in vivo* model.
- We have filed a disclosure and are moving to patent this material.
- We are currently assembling the first manuscript describing this technology.
- Our next goal is to implement the material *in vivo*.

Task 3: To achieve rapid bone formation by percutaneous injection of the encapsulated Ad5F35BMP2 transduced human bone marrow mesenchymal stem cells (hBM-MSCs) into the adjacent musculature of athymic rats in a model of nonunion.

- We have established and set up a reproducible critical size defect model that due to the nature of the site is a tremendously challenging model of bone healing.
- We have demonstrated the ability to transduce both the human cells to express high levels of BMP2, as well as the rat fibroblasts, which we believe to be genetically matched donors.
- We have initially tested the BMP2 transduced cells to induce both heterotopic bone formation and bone healing in this model and found that heterotopic ossification can be rapidly produced in an immune compromised animal using transduced human fibroblasts expressing high levels of BMP2.
- We have found that we are not able to induce heterotopic ossification or bone healing in the wild type rats, and are currently following up on this to determine if our current cell line is an adequate genetic match for the rats. Our data, in separate experiments pertaining to the spine, clearly demonstrated the ability to form rapid bone formation similarly in both immune competent and incompetent models. Therefore most likely this is a problem with the rat cells and model, rather than an issue with the gene therapy system itself, but something we must keep in mind when we develop this for clinical use for the general population.
- We are currently continuing to trouble shoot the production of bone formation from the biomaterial, so that we can target the formation more appropriately to allow for rapid healing of the defect. This will involve not only introducing the biomaterial in vivo, but also analyzing the placement of the material

within the defect. We have on going studies in the spine, which demonstrate the need for appropriate placement of the cells and biomaterial for optimal targeting.

Reportable Outcomes:

This past year we have collected data for two manuscripts. The first is in review (see appendix) and demonstrates the presence of new vessels prior to the appearance of cartilage. This manuscript also demonstrates the up-regulation of VEGF's by our gene therapy system. The second manuscript describes the optimization of the selectively degradable hydrogel material based on the principles of bone remodeling. This work demonstrates the ability of osteoclasts to resorb the hydrogel similarly to bone.

I presented the work at the American Society of Gene Therapy Annual Meeting in Boston MA, May 28th-June 1st.on the research in the laboratory including the development of this gene therapy system for healing critical size defects. We have also submitted an abstract for poster presentation on this work. We have also presented this work at the 7th Annual BMP2 meeting in Lake Tahoe CA, in a poster format. The work has been presented within Baylor College of Medicine at the Annual Center for Cell and Gene Therapy Retreat. The project was both highlighted in an oral presentation as well as a poster format.

Dr. Ronke Olabisi, who is a post-doctoral fellow in Dr. Jennifer West's laboratory, will present her work on the degradable hydrogel at the Society for Biomaterials 2009 Annual Meeting and Exposition: *Giving LIFE to a world of materials,* April 22 - 25, 2009 in San Antonio, Texas, USA. Dr. Olabisi's work was selected for an oral presentation at the meeting. We have currently been asked to present the work at both the upcoming American Society of Bone and Mineral Research meeting (ASBMR) small topical meeting on Brain, Bone, Fat and Nerves, in Bethesda and the 4th Annual New York Skeletal Society in New York City both at the end of April. We will submit both oral and poster presentations at these meetings. Finally have will present two posters at the upcoming Orthopedic Research Society Annual Meeting. The work described in the abstract highlights the work on both developing the model as well as highlighting the recent developments of the BMP2 gene therapy system in combination with the hydrogel material.

Finally we have filed two disclosures describing first the gene therapy system and are moving towards patenting this system for the use of heterotopic ossification for the healing of critical size defects, and secondly the osteoclast specific degradable PEG-DA hydrogel material.

Conclusions:

We have made significant progress for this second year of the four year proposed study. In the upcoming years we hope to complete the studies described in aim 1, using the BMP2- DSRed vectors to compare temporal and spatial expression of BMP2 on endochondral bone formation. We are currently completing and publishing the *in vitro* phase for developing the osteoclast degradable hydrogel material, through the principles of bone remodeling. Finally we have not only established a challenging model of non-union critical size defects in rats, but also have preliminary data that BMP2 is capable of healing or producing bone under these circumstances. Although we have just started this work the rapid new bone within two weeks, and the large amount of new bone filling the defects, suggests the gene therapy based system holds much promise. We believe in the upcoming year that we will further optimize this system to obtain the rapid and complete healing of the defect. Further, we will determine if this is due to heterotopic bone formation fusing into the orthotopic, or stimulation of the orthotopic bone by BMP2 to induce healing. We will start to test the biodegradable hydrogel structures in the critical size defect model. We will also optimize the placement of the biomaterial for optimal healing. Since ultimately this material will be injectable, we want to determine the number of injections and exact locations for optimal healing. We would like to introduce a second model for critical size defect in the tibia, in which we will fix the bone by plating, and thus allow for us to compare our healing in the fibula to that in a more weight bearing bone. Thus we have considerable challenges in the third year of this proposal, but have had significant achievements in the first two years, to develop the tools necessary for completing the experiments. In accordance with our projected timeline we are exactly on schedule. Thus the substantial preliminary data, from the first two years, suggests success in our endeavors.

References:

1. Gowen, M., et al. (1999). Cathepsin K knockout mice develop osteopetrosis due to a deficit in matrix degradation but not demineralization. *J Bone Miner Res* 14: 1654-1663.
2. Hollberg, K., Nordahl, J., Hultenby, K., Mengarelli-Widholm, S., Andersson, G., and Reinholt, F. P. (2005). Polarization and secretion of cathepsin K precede tartrate-resistant acid phosphatase secretion

to the ruffled border area during the activation of matrix-resorbing clasts. *J Bone Miner Metab* 23: 441-449.
3. Yang, F., Williams, C. G., Wang, D. A., Lee, H., Manson, P. N., and Elisseeff, J. (2005). The effect of incorporating RGD adhesive peptide in polyethylene glycol diacrylate hydrogel on osteogenesis of bone marrow stromal cells. *Biomaterials* 26: 5991-5998.
4. Fouletier-Dilling, CM. et al. (2005). Novel compound enables high-level adenovirus transduction in the absence of an adenovirus-specific receptor. *Hum Gene Ther* 16: 1287-1297.
5. Fouletier-Dilling CM, Gannon F, Olmsted-Davis EA, Lazard Z, Heggeness MH, Shafer JA, Hipp JA, and A.R. Davis. (2007) Efficient and Rapid Osteoinduction in an Immune Competent Host. Hum Gene Ther 18(8):733-45 (Fast Track publication and Cover).
6. Olmsted-Davis, EA, *et al.* (2002). Use of a chimeric adenovirus vector enhances BMP2 production and bone formation. *Hum Gene Ther* 13: 1337-1347.
7. Bikram M, Fouletier-Dilling CM, Hipp JA, Gannon F, Davis AR, Olmsted-Davis EA, and West JL (2007) Endochondral Bone Formation from Hydrogel Carriers Loaded with BMP2-Transduced Cells. Ann Biomed Eng. 35(5):796-807.
8. Olmsted, EA. *et al.* (2001). Adenovirus-mediated BMP2 expression in human bone marrow stromal cells. *J Cell Biochem* 82: 11-21.
9. Gugala, Z., Davis, A.R., Fouletier-Dilling, C, F. Gannon, Lindsey, R.W., Olmsted-Davis, EA (2007) Adenovirus BMP2-Induced Osteogenesis in combination with various collagen carriers. Biomaterials, 28(30):4469-79.

Appendix:

- **Manuscript entitled " Vessel Formation is Induced Prior to the Appearance of Cartilage in BMP2-mediated Heterotopic Ossification"**

Vessel formation is induced prior to the appearance of cartilage in BMP2-mediated heterotopic ossification

C. Fouletier Dilling[1], A. M. Wada[2], M. Merched-Savage[1], Z.W. Lazard[1], F.H. Gannon[3], T. J. Vadakkan[2], L. Gao[2] , K. Hirschi[1,4], M.E. Dickinson[2], A.R. Davis[1,5], E.A. Olmsted-Davis[1,5]

[1]Center for Cell and Gene Therapy, Baylor College of Medicine, Houston, TX
[2]Department of Molecular Physiology, Baylor College of Medicine, Houston, TX
[3]Department of Pathology, Baylor College of Medicine, Houston TX
[4]Department of Pediatrics, Pediatrics-Nutrition, Baylor College of Medicine, Houston, TX
[5]Department of Pediatrics, Hematology-Oncology, Baylor College of Medicine, Houston, TX

Funded in part by RO1EB005173-01, USMRMC 06135010 and USMRMC 06136005

Running title: Vessels form prior to cartilage

cdillingdk@yahoo.com, wada@bcm.tmc.edu, mms@bcm.tmc.edu, zwl@bcm.tmc.edu, fgannon@bcm.tmc.edu, vadakkan@bcm.tmc.edu, liangg@bcm.tmc.edu, mdickins@bcm.tmc.edu, khirschi@bcm.tmc.edu ardavis@bcm.tmc.edu, edavis@bcm.tmc.edu

Corresponding Author
Elizabeth A. Olmsted-Davis
Center for Cell and Gene Therapy
One Baylor Plaza
Houston, TX 77030
Ph 713-798-1253
Fax 713-798-1230
edavis@bcm.tmc.edu

Word count: 37,142
Abstract: 237
Manuscript: 36,905

Number of figures:10
Black and White: 2
Color: 8

All authors have no conflicts of interest

Abstract

Heterotopic ossification (HO) or endochondral bone formation at non-skeletal sites, often results from traumatic injury, and can lead to devastating consequences. Alternatively the ability to harness this phenomenon would greatly enhance current orthopedic tools for treating segmental bone defects. Thus understanding the earliest events in this process would potentially allow us to design more targeted therapies to either block or enhance this process. Using a murine model of HO, we identify one of the earliest stages in this process to be the establishment of new vessels prior to the appearance of cartilage condensations. This model relies on the production of HO by delivery of adenovirus transduced cells expressing bone morphogenetic protein 2, BMP2.

As early as 48 hours after induction of HO, we observed the appearance of brown adipocytes expressing VEGFs, simultaneous to the peak of endothelial cell replication. To further characterize if these observed changes correlated with new vessel formation, we utilized mice possessing a cassette consisting of the VEGF receptor 2 (flk-1) promoter driving the expression of nuclear-localized yellow fluorescent protein (YFP). This marker has previously been shown to correlate with newly established vasculature. Quantification of the flk-YFP^{+} showed a significant increase in YFP expression as compared to the control. The establishment of new vessels occurred two days prior to the influx of chondrocytic progenitors. The data collectively suggests that vascular remodeling and growth maybe essential for engrafting the necessary progenitors to form endochondral bone.

Introduction

Endochondral bone formation is thought to proceed through an ordered series of events, starting with the proliferation and "condensation" of presumptive mesenchymal cells to form avascular cartilage. Hence it is presumed that the lack of vasculature and associated cellular replication creates the hypoxic environment necessary for chondrogenic differentiation. However, recent data from our laboratory using a model of heterotopic ossification, suggests that vessels may play an essential role in the induction of chondrogenesis.

It has been well established that vessel formation plays a key role in the process of bone formation, through the invasion of perichondrium and hypertrophic zone and is required for the replacement of cartilage by bone (1). The angiogenic factor, vascular endothelial growth factor (VEGF) promotes vascular invasion via specifically localized receptors, including Flk expressed in endothelial cells in the perichondrium or surrounding tissue (2) (3). These events of cartilage matrix remodeling and vascular invasion are necessary for the migration and differentiation of osteoblasts and osteoclasts which remove mineralized cartilage matrix and replace it with bone. However, much less is known about the role of vessel formation prior to the appearance of the pre-cartilage.

During normal wound repair, a series of factors are believed to be induced by the hypoxic state of the tissues, resulting in up-regulation of hypoxia inducible factor (HIF) that in turn up-regulates a series of factors including VEGF that lead to vessel formation. This early angiogenesis has been proposed to be necessary

for creating the specialized vessels essential to progenitor homing and engraftment into the damaged tissues (4). Little is known as to whether such a process plays a key role in the repair of bone.

Using a model of *de novo* bone formation to identify the earliest events in this process, we have demonstrated that myelo-mesenchymal stem cells are recruited to the tissues to form the early cartilage (5). One of the earliest events in this model is the appearance of brown adipocytes. These cells are capable of utilizing their uncoupled aerobic respiration to reduce localized oxygen tension and effectively pattern the newly forming cartilage condensations (6). This is consistent with *in vitro* data where bone marrow derived mesenchymal stem cells can undergo chondrogenesis in the presence of bone morphogenetic protein 2 (BMP2) and low oxygen (7). Thus, these progenitors may indeed be recruited to the site of new bone formation through the vasculature. In this study we focused on defining the role of early vessel formation in endochondral bone induction prior to the appearance of the mesenchymal condensations.

To determine whether new vessel formation precedes the appearance of cartilage at the BMP2 induction site, we chose to employ a transgenic mouse model which expresses the fusion protein, human histone H2B with enhanced yellow fluorescent protein (EYFP) (H2B:YFP) in endothelial cells under the regulation of flk1 promoter/enhancer fragment (Flk1-H2B::YFP)(8). Recent improvements in genetically encoded fluorescent protein expression in animal models along with the advances in optical imaging and development of images analysis software have become powerful tools for studying many aspects of

tissue development cellular level (9). Previous studies using this transgenic animal suggest that Flk1-H2B::YFP expression is restricted to endothelial cells of smaller and/or newly forming vessels (8), thus providing a mechanism for quantification of new vessels.

Here we demonstrate new vessel formation within the tissues prior to the appearance of the presumptive cartilage. Quantification of the number of endothelial cells shows that one of the first steps of bone formation is to induce additional endothelial cells to build new vessels. Histological analysis suggests that this is indeed an earlier wave of angiogenesis within the tissues, just prior to the influx of chondrocytic progenitors. Microarray and immunohistochemical analysis of the tissues prior to the mesenchymal condensations, revealed a rapid and transient expression of VEGFA and D from the brown adipocytes. The data collectively, suggests that the brown adipocytes may play a key role in establishing patterning of the cartilage through regulation of oxygen tension within the tissues, through induction of both aerobic respiration, as well as early angiogenesis.

MATERIALS AND METHODS

Cell culture: A murine C57BL/6 derived cell line (MC3T3-E1) was obtained from American Type Culture Collection, propagated in αMEM supplemented with 10% fetal bovine serum (Hyclone, Logan, UT), 100 units/ml penicillin, 100 μg/ml streptomycin, and 0.25 μg/ml amphotericin B (Life Technologies Inc., Gaithersburg, MD). Briefly, the cells were grown in DMEM supplemented as

described above and cultured at a subconfluent density in order to maintain the phenotype. All cell types were grown at 37°C and 5% CO_2 in humidified air.

Transduction of cells with adenovirus in the presence of GeneJammer®

Adenoviruses**:** Replication defective first generation human type 5 adenovirus (Ad5) deleted in regions E1 and E3 was constructed to contain cDNAs for BMP2 in the E1 region of the viral genome (9). The virus particles (vp) to plaque forming units (pfu) ratio were: 55 and 200 for Ad5BMP2 and Ad5-empty respectively, and all viruses were shown to be negative for replication competent adenovirus.

The C57BL/6 cell line or MC3T3-E1 (1×10^6), were transduced with Ad5BMP2 or Adempty cassette control virus at a concentration of 5000 vp/cell with 1.2% GeneJammer® as previously described (10). Briefly, 15μl of GeneJammer® or PBS was added to 500μl of αMEM medium without supplements and incubated for 10 minutes at room temperature. The virus was then added at the indicated concentrations and the mixture further incubated for 10 minutes at room temperature. This virus-GeneJammer® mixture was added to approximately 1×10^6 cells along with 750 μl of αMEM containing 10% fetal bovine serum (Hyclone, Logan, UT), 100 units/ml penicillin, 100 μg/ml streptomycin, and 0.25 μg/ml amphotericin B (Life Technologies Inc., Gaithersburg, MD). The cells were incubated at 37°C for 4 hours and then the mixture was diluted with 3 ml of fresh media containing FBS.

Heterotopic bone assay: The transduced cells were resuspended at a concentration of 5 x 10^6 cells/100 µl PBS, and then delivered through intramuscular injection into the hind limb quadriceps muscle of Flk1 mice. Animals were euthanized at daily intervals and hind limbs were harvested, embedded and placed at -80°C. All animal studies were performed in accordance with standards of the Baylor College of Medicine, Department of Comparative Medicine after review and approval of the protocol by the Institutional Animal Care and Use Committee (IACUC).

Histological analysis and staining analysis:

Soft tissues encompassing the site of new bone formation were isolated from the rear hind limb of the mice. Both the skin and skeletal bone were removed from the tissues prior to freezing. Serial sections (15 µm) were prepared that encompassed the entire tissues (approximately 50 sections per tissue specimen). We then performed Hematoxylin and Eosin staining on every 5^{th} slide which allowed us to locate the region containing either our delivery cells or the newly forming endochondral bone.

Serial unstained slides were used for immunohistochemical staining (either single or double-antibody labeling). For double antibody labeling, samples were treated with both primary antibodies simultaneously followed by washing and incubation with respective secondary antibodies, used at 1:500 dilution to which Alexa Fluor 488, 594 ,or 647 were conjugated. Primary antibodies were used as follows: SMA mouse monoclonal used at 1:200

dilution; Sigma), CD31 (rat monoclonal used at 1:75 dilution; BD Pharmingen), Flk1 (goat polyclonal used at 1:100 dilution; R&D systems), Ki67 (rat monoclonal used at 1:100DakoCytomation, DK), Histone H3 (mouse monoclonal used at 1:100 dilutionMillipore Corporation), VEGF-D (goat polyclonal used at 1:100 dilutionSanta Cruz Biotechnology, INC). Stained tissue sections were examined by confocal microscopy (Zeiss LSM 510 META) using a 20x/0.75NA objective lens.

Flk1 positive cell quantification in Bmp induced tissues: To quantify the increase in YFP positive cells in the BMP induced tissues,frozen sections across these tissues were counterstain with DAPI and the YFP expression was compared to that obtained in the control tissues. First, a series of low magnification (5.4x and 12x) bright field images of a tissue section were taken and overlapped to reconstruct the tissue section using Adobe Photoshop CS3. The reconstructed montage image was used to measure the area of the tissue section using a manual contour tracing method (Zeiss Axiovision). The area of each of the frozen sections was calculated in a similar manner. Area measurements are used to determine the density of labeled cells as indicated below.

High resolution (10X/NA0.45, 1024x1024 pixels), dual channel images of tissue sections nuclear stained with DAPI were taken using a confocal microscope (Zeiss LSM 510 META). In each image, the number of nuclei in the DAPI and YFP channels was counted using a modified watershed segmentation

algorithm (FARSIGHT, RPI) which makes use of both intensity and volume thresholds to distinguish two nuclei as separate. All the nuclei counted using the software were DAPI positive. The fraction of DAPI stained nuclei marked by YFP were counted as YFP positive nuclei. The density of YFP positive cells in a tissue section was defined as the ratio of the number of YFP positive nuclei in the tissue section measured from the high magnification images to the area of the tissue section measured from the low magnification images. The density of the YFP positive nuclei was calculated for a number of control and BMP treated tissues at 2 and 4 days after injection. The ratios were then averaged over the various control and BMP2-treated tissues. The p- values were calculated using a Student's t-test (MS Excel).

Flk1-YFP positive cell association analysis:

To characterize the cell type(s) that express YFP in the adult muscle tissue, we performed immunoflourescent studies using endothelial cell marker CD31 and Flk1 antibodies; for vascular smooth muscle cells -smooth α actin (SMA). Association of cells expressing YFP with immunolabeled cells was analyzed using (FARSIGHT, RPI, NY) and a custom program written in MATLAB (MathWorks, Natick, MA). After identification of each nucleus by DAPI staining, YFP positive and negative cells were then analyzed for association with fluorescent signals of each antibody. An intensity threshold was applied to the red channel in each image to identify a cell positive or negative for the immunofluorescent signal. Each identified nucleus and overlapping red channel

were counted as CD31, Flk1, or SMA positive and then as either YFP negative and positive. Co-localization percentages are shown in the supplemental data section (Table S-1) and describe in detail the YFP positive cell types.

Q-RT-PCR: Non-skeletal tissues (n=4 per group) surrounding the site of injection of the AdBMP2 or Ad control transduced cells were isolated daily over the seven day period of bone formation and prepared as total RNA using a Trizol reagent in accordance with the manufacturer's specifications. The two groups of RNAs were subjected to Q-RT-PCR analysis in parallel and the Ct values obtained normalized to both internal 18S ribosomal RNA used in multiplexing, and to each other to remove changes in gene expression common to both the BMP2 and control tissues by using the method of $\Delta\Delta$Ct along with Taqman® primers and probes (Applied Biosystems) as previously described (6).

RESULTS

Upregulation of vessel markers prior to the onset of chondrogenesis: We have previously described a model of rapid endochondral bone formation (11) in which mineralized bone is observed approximately seven days after the initial induction with BMP2. Due to the rapid nature of model, we examined tissues at 24 hour intervals over the period leading up to chondrogenesis (day 5) to characterize the presence or absence of new vessel formation within these tissues. Frozen sections were immuno-stained to determine if endothelial cells were undergoing replication. Figure 1 shows the results of co-immuno-staining

for the endothelial cell specific factor, von Willibrand factor (VWF) (red) and Ki-67 (green), a marker of cellular replication (12). As can be seen in figure 1, there is extensive cellular replication within the tissues on all days, however, the peak of replicating VWF+ cells was observed on day 2, supporting the microarray findings that suggest endothelial cell replication is one of the first stages of the new bone formation. Higher resolution images) taken using confocal microscopy (see Materials and Methods) confirm that the apparent overlapping expression of VWF and the replication marker Ki67 is within the same cell (Figure 1, bottom panel). Endothelial cell replication appeared to be complete by four days after initial induction and just prior to the start of chondrogenesis (day 5, (13)).

Vascular Endothelial Growth Factor (VEGF) mRNA expression:

The peak of endothelial cell replication appears to coincide with the significant elevation in the vascular endothelial growth factor, VEGF-D (also termed fos-induced growth factor, FIGF) on the second day after injection of BMP2-producing cells as determined by preliminary microarray analysis (data not shown). To confirm the elevation in VEGF-D and further quantify the expression profile of the other three family members (VEGF-A, -B, -C) over the early stages of endochondral bone formation, RNA harvested from tissue at the induction site was subject to quantitative reverse transcription PCR (Q-RT-PCR). Figure 2 show the changes in VEGF mRNA expression from day 1 after injection of BMP2-producing cells until day 6. There is a significant increase in VEGF-A and VEGF-D mRNA expression at days 2 and 4. VEFG-B and VEGF-C however

remain on the same level throughout the time course. Although the data cannot differentiate between expansion of cells expressing VEGF-A and –D, and elevated transcription within cells residing in the area, the results suggest that these potent endothelial growth factors are rapidly and transiently increased within the site of new bone formation prior to the onset of cartilage.

Flk1-H2B::eYFP in vessels:

We next wanted to determine if the observed replication and elevation in VEGF-A and D resulted in an increased number of endothelial cells at the bone induction site prior to chondrogenesis, consistent with new vessel formation. We chose to utilize the Flk1-H2B::eYFP mouse model(8), in which new vessel formation could be readily quantified within the muscle tissues. Flk1 is a VEGF receptor transiently expressed on endothelial cells, and is presumably thought to contribute to VEGF induced endothelial cell replication (14). Therefore quantification of the YFP expression within tissues from animals receiving either transduced cells expressing BMP2 or control allows us to determine in new vessels were being established and to quantify increases in the number of endothelial cells within the muscle prior to cartilage.

Frozen sections were prepared by serial sectioning from Flk1-H2B::eYFP adult hind limb soft tissue (n=4 per group) consisting of three groups, those receiving: (1) cells transduced with Ad5BMP2, (2) cells transduced with Ad5empty cassette control virus, and (3) normal mouse muscle. To ensure uniform quantification and adequate sampling for quantification, the entire region

of soft tissues in the hind limb was frozen sectioned, and approximately ever fifth section was for analyzed for YFP expression.

As can be seen in Figure 3 both treated and control tissues possessed flk1+ cells. To quantify differences in the number of endothelial cells, the number of YFP+ per the total number of DAPI+ cells was determined using automated segmentation methods (see Materials and Methods). The total number of YFP+ cells was also determined for the total area of the tissue section to ensure there was no bias in the fields of view chosen for image analysis (see Materials and Methods).The total number of Flk1+ cells were quantified in tissues isolated from both BMP2 and control mice.   Since VEGF expression appears to be transient within the tissues, we analyzed tissues isolated on days 2 and 4 after delivery of the transduced cells, corresponding to the biphasic peaks of the VEGF expression observed above (Figure 2). Figures 3A and 3B represent the montages of the tissue receiving Ad5BMP2 or Ad5empty cassette transduced cells, respectively. Figure 3B show a significant increase in the number of areas with Flk1+ cells. Flk1-YFP+ cells seems scattered along the vessels in the controls sections while in the BMP2 montage the Flk1+ cells appears to be present in a more organized pattern.

Figure 4 shows the results of this analysis of the tissues isolated 2 and 4 days after induction of bone formation with the transduced cells. The total number of Flk1+ cells per unit area were counted and quantified. Figure 4 shows the average number of Flk1+ cells on day 2 and day 4. The quantification of the Flk1-YFP+ in tissues isolated from either the region receiving cells transduced

with either Ad5BMP2 or a control adenovirus, showed a significant increase in the number of YFP+ cells as compared to the control within two days after induction. Analysis of the entire soft tissues within several mice showed a two-fold elevation after induction of bone formation with BMP2. This 2 fold induction was shown to be significant (p=0.017, day 2 (Fig 4A) and p=0.006, day 4 (Fig 4B) as compared to the control, on both days 2 and 4. The peak was approximately 2 days after induction of bone formation with no statistically significant difference between these results and those obtained in tissue sections isolated 4 days after induction. The continued elevation of flk-1 positive cells from day 2 to day 4 suggests the continued expression of the marker in cells that expanded on day 2. This data is consistent with our observation (figure 1) that endothelial cell replication peaks 2 days after delivery of the BMP2 transduced cells and is completed within the four day period.

Flk1+ cells are associated with vessels and replicating endothelial cells:

To further confirm that these Flk1-H2B::eYFP cells are replicating endothelial cells we co-immuno-stained these sections for the presence of the endothelial cell marker CD31, and the replication marker Histone H3 (HH3). As can see in figure 5A, the flk1-YFP+ cells are replicating and are associated with the CD31 marker while on the control sections, the flk1-YFP+ cells are associated with CD31 but the cells are disperse and non-replicating. Both tissues are representative of what we observed in tissues isolated 48 hours after delivery of either the Ad5BMP2 (5A) or Ad5empty (5B) transduced cells.

Role of brown adipose in vessel formation:

The data collectively confirms that vessel replication is occurring simultaneously with elevated expression of VEGFs within the tissues. However, we cannot determine if this enhanced VEGF expression is within pre-existing cells within the tissues that are transcriptionally upregulating expression of this protein, or whether new cells are expanding within the region. Since one of the earliest events observed in our model, is the recruitment and expansion of brown adipocytes (6)we next chose to determine if these cells might be expressing the VEGFs. Immunohistochemical analysis of frozen sections from the Flk1-YFP animals injected with Ad5BMP2 or Ad5empty cassette transduced cells showed co-localization of VEGF-D (green color) and the brown adipocyte specific marker uncoupling protein 1 (UCP1; red color) (day 2). As can be seen in Figure 6, the expression of UCP1 overlaps expression of VEGF-D and is adjacent to the Flk1+ endothelial progenitors, suggesting that the brown adipocytes may be responsible for regulating the new vessel formation.

Discussion

Similar physiological steps lead to bone formation during embryonic development and in adult organisms, for instance in fracture repair or heterotopic ossification. In both cases, bone formation begins with mesenchymal condensations and ends with maturation of the growth plate, recruitment of osteoblasts and the production of bone. Vascularization has been shown to play

a critical role in this process, through the infiltration into cartilage to form vascularized bone. Here we present data that show that vessels play a much earlier role in patterning of the cartilage and bone. The results show the presence of new vessel formation prior to the onset of mesenchymal condensations and cartilage.

We have previously reported the presence of brown adipocytes within the tissues, two days after the initial induction. We have also shown that these cells regulate localized oxygen tension through their unique metabolism (6). In this study we extend our knowledge of the functional role of brown adipocytes, to include their rapid and transient expression of the potent angiogenic factors VEGF-A and –D. Interestingly a similar rapid and transient expression of VEGF-D has also been demonstrated in limb development and shown to be critical for patterning (15). Our data collectively suggests that the brown adipocytes may induce the synthesis of new vessels, as a component for patterning the newly forming cartilage. In the proposed model, the brown adipocytes induce new vessels, facilitating the recruitment of chondrogenic precursors, while at the same time lowering localized oxygen tension to allow for chondrogenic differentiation. In support of this mechanism, we show in this study, the presence of brown adipocytes, expressing VEGF-D only in areas adjacent to our newly expanding vessels as marked by Flk1-H2B::YFP.

Using a model of rapid endochondral bone formation, we show the immediate expansion of vessels within the tissues in response to delivery of BMP2. Although BMP2/4 play a critical role in the patterning of cartilage and

bone in the embryo (16)[i], much evidence now links the bone morphogenetic proteins to a host of other earlier physiological functions including vascularization of the early embryo (17) In the embryo BMPs have been implicated in neural induction   Thus it may not be surprising that the earliest stage of bone formation in our model is the induction of new vessel formation.

Upon BMP2 stimulation, the Flk-1 endothelial progenitors expand in both total number of positive vessels as well as the total number of cells per vessel. The expansion of the flk1 positive cells correlated well with the results of the immunohistochemical analysis. Endothelial cell replication peaked within 2 days after induction with BMP2, while no endothelial cell replication was noted in the tissues receiving cells transduced with the control vector.   In these studies endothelial cells were confirmed by using both CD31 and VWF and replication was determined by positive expression of two different proteins associated with cellular replication (Ki-67, and HH3). Upon higher magnification imaging, we observed entire small vessels undergoing replication. However the Flk 1-YFP cells appear to be clustered in the middle of the small vessels, on only a subset of the CD31 positive endothelial cells, suggesting a more transient nature for the expression of this marker. Thus the transient nature of the Flk-1 expression suggests that the calculated induction with BMP2 may in fact be an under representation of the true difference. The data collectively, shows the immediate up regulation of new vessel formation through expansion of endothelial cells in the tissues in response to BMP2.

Vascular endothelial growth factors (VEGFs) have been shown to be essential to expansion of both endothelial cells as well as vascular smooth muscle cells which assemble to form the vessel structure. Although VEGFA has been most commonly shown to be responsible for angiogenesis in most systems, recent studies in murine muscle have found VEGF-D to an extremely potent angiogenic factor (18). This family member is better known for its critical role in the expansion of lymphatic vasculature (18). In our model we see both factors highly expressed in the tissues receiving the BMP2 transduced cells, as compared to those receiving control cells. Again the rapid but transient elevation in VEGF expression suggests that these factors may be driving the endothelial cell replication. Perhaps the increase in both VEGFs suggests that both new vasculature and new lymphatics are being established in the tissues. We and others have recently shown the chondrocyte to be of myeloid original, which circulates to the site of new bone formation. These cells must then recruit and pass from the vessels into the tissues, through a process of known as stem cell extravasation. This process has been shown to require small vasculature, which has a reduced blood flow. Thus it is conceivable that brown adipocytes express the VEGFs to form new vessels, capable of permitting recruitment of chondrocytic progenitors to the correct location for endochondral bone formation. Since vascular invasion of the growth plate has been well documented as a mechanism for recruiting osteoblast progenitors to form the new bone, it would not be surprising to have an earlier phase of this process that recruited the chondrocytic progenitors.

We have previously shown that the brown adipocytes are capable of inducing hypoxia in the local environment which in the presence of BMP2 has been shown to induce chondrogenesis (6). Thus we propose that the brown adipocytes are capable of patterning the newly forming cartilage by inducing new vessel formation, while simultaneously removing oxygen through uncoupled aerobic respiration. Once the progenitors differentiation into chondrocytes, they then express a number of anti-angiogenic proteins, to prevent in growth of new vessels, thus momentarily attenuating this early wave of angiogenesis.

Thus the results presented in this study extend our knowledge about the critical nature vascularization plays not only in bone formation but in cartilage as well. The data collectively shows a novel process for patterning of new endochondral bone, in adult organisms. Further, this is one of the first studies that attempts to understand the biology of tissue engineering of cartilage. Surprisingly one of the critical components we have identified is contradictory to our current dogma, that cartilage does not require vessels. Hence the work greatly advances our knowledge which is essential to our efforts to replace damaged cartilage through tissue engineering.

Figure Legends:

Figure 1: Immunohistochemical analysis of endothelial cell replication in tissues isolated at daily intervals after induction of bone formation with cells expressing BMP2. A-D; days1, 2, 3 and 4, respectively, after injection of BMP2-producing cells, paraffin sections were prepared and stained with an antibody against Ki67 followed by as secondary antibody conjugated to Alexa fluor 547 (red) mixed with an anti-Von Willibran Factor (VWF) antibody followed by a secondary antibody conjugated to Alexa fluor 488 (green).

Figure 2: Expression of VEGF-D during the early stages of endochondral bone formation. Results of real time quantitative RT-PCR analysis of *VEGF- A,-B,-C, and -D* mRNA levels in tissues surrounding the lesional site that received either the Ad5F35BMP2- or Ad5F35empty cassette-transduced cells isolated at daily intervals for up to 7 days after initial injection. Samples were run in triplicate and the averages normalized against those obtained from the tissues receiving cells transduced with Ad5F35empty cassette virus. Therefore the graph depicts the fold changes in VEGF RNA's in the BMP2 samples over time as compared to the control tissues.

Figure 3: Representative image of tissue section isolated 2 days after injection of cells transduced with **(A)** AdBMP2 or **(B)** AdEmpty cassette in grayscale. High resolution confocal images of various areas (a1-a20) for the samples receiving BMP2 or (a1-a4) for tissues receiving cells transduced with the control

adenovirus were taken in RGB images. The total number of YFP positive cells in the tissue was counted by adding the number of YFP positive cells in each of the high resolution images. The arrows point to regions in the tissue where the high resolution images were taken.

Figure 4: Average number of flk1-YFP+ cells per unit area of the tissue which received cells transduced with Ad5BMP2 were normalized to those receiving cells transduced with Ad5empty cassette. Sections from two independent samples were generated from representative tissues, that encompassed the entire hind limb and then the flk1-YFP+ cells were quantified. A significant increase in the density of Flk1+ cells was observed on **(A)** Day 2 and **(B)** Day 4.

Figure 5: Immunohistochemical analysis of the Flk1-H2B::YFP mouse tissues to determine if the flk-yfp+ (yellow) are replicating. Tissues were isolated from 2 days after receiving cells transduced with **(A)** Ad5BMP2 or **(B)** Ad5Empty cassette vector, and immunostained for the replication marker Histone H3 (HH3, green) and the endothelial cell marker CD31 (red). Cells were counterstained with dapi. Representative images are depicted.

Figure 6: Immunohistochemical staining for brown adipocytes expressing VEGFD (green color) in tissues isolated from the Flk1-H2B::YFP mice 4 days after receiving cells transduced with Ad5BMP2.   Brown adipocytes were identified as cells expressing uncoupling protein 1 (UCP 1; red color) and the

yellow color represents the Flk-yfp+ endothelial cells within the muscle. Tissues were counterstained with dapi (blue color) that stains the nucleus of cells.

Figure 1:

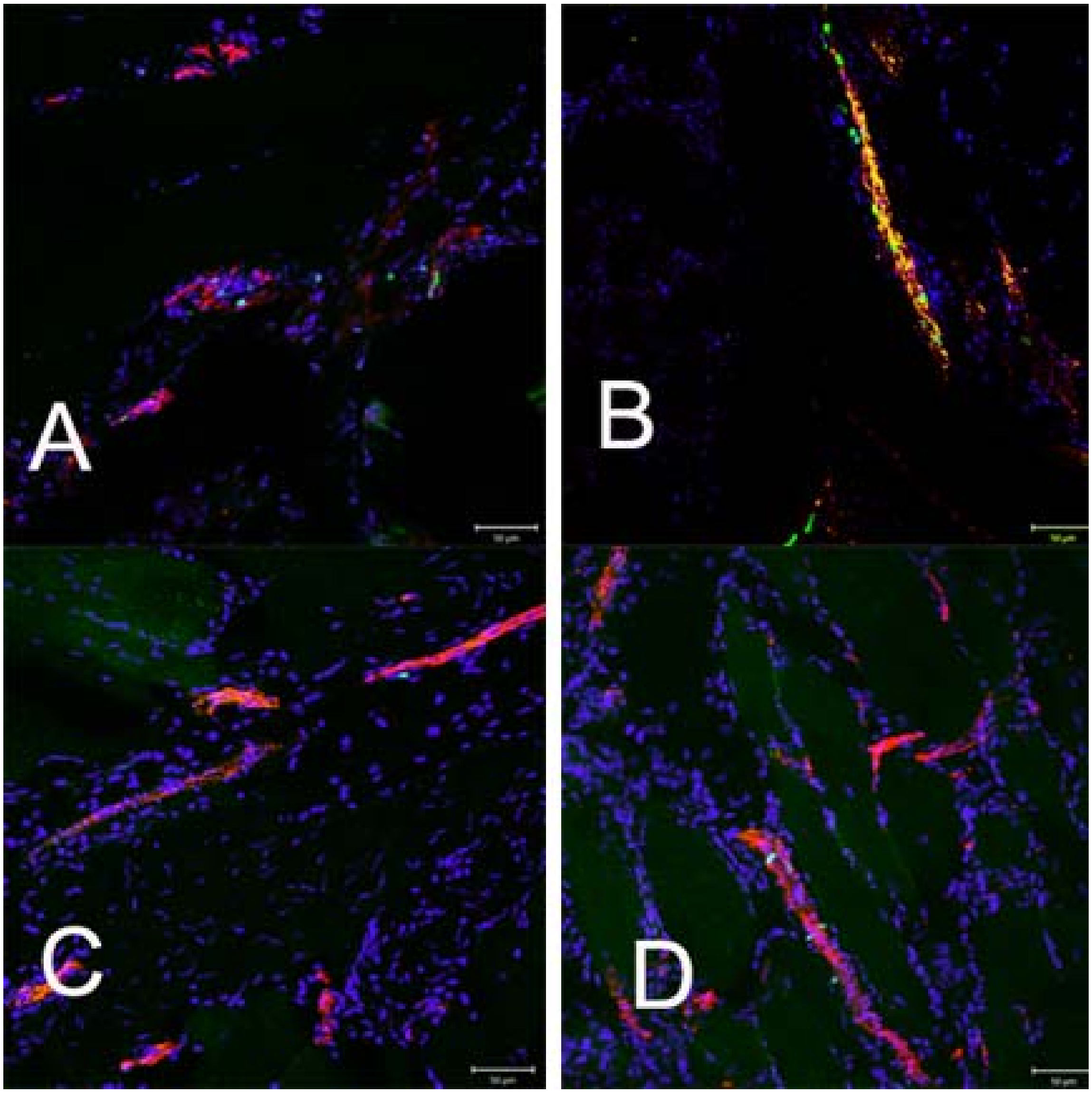

Figure 2:

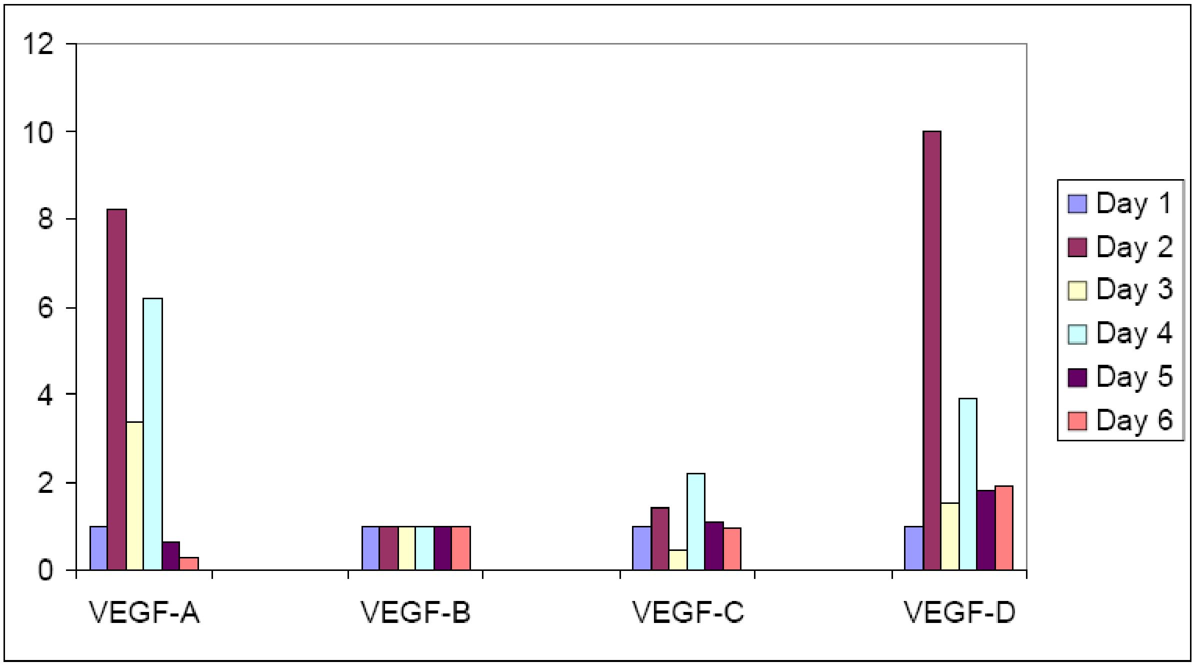
12
10
8
6
4
2
0
VEGF-A
VEGF-B
VEGF-C
VEGF-D
Day 1
Day 2
Day 3
Day 4
Day 5
Day 6

Figure 3A:

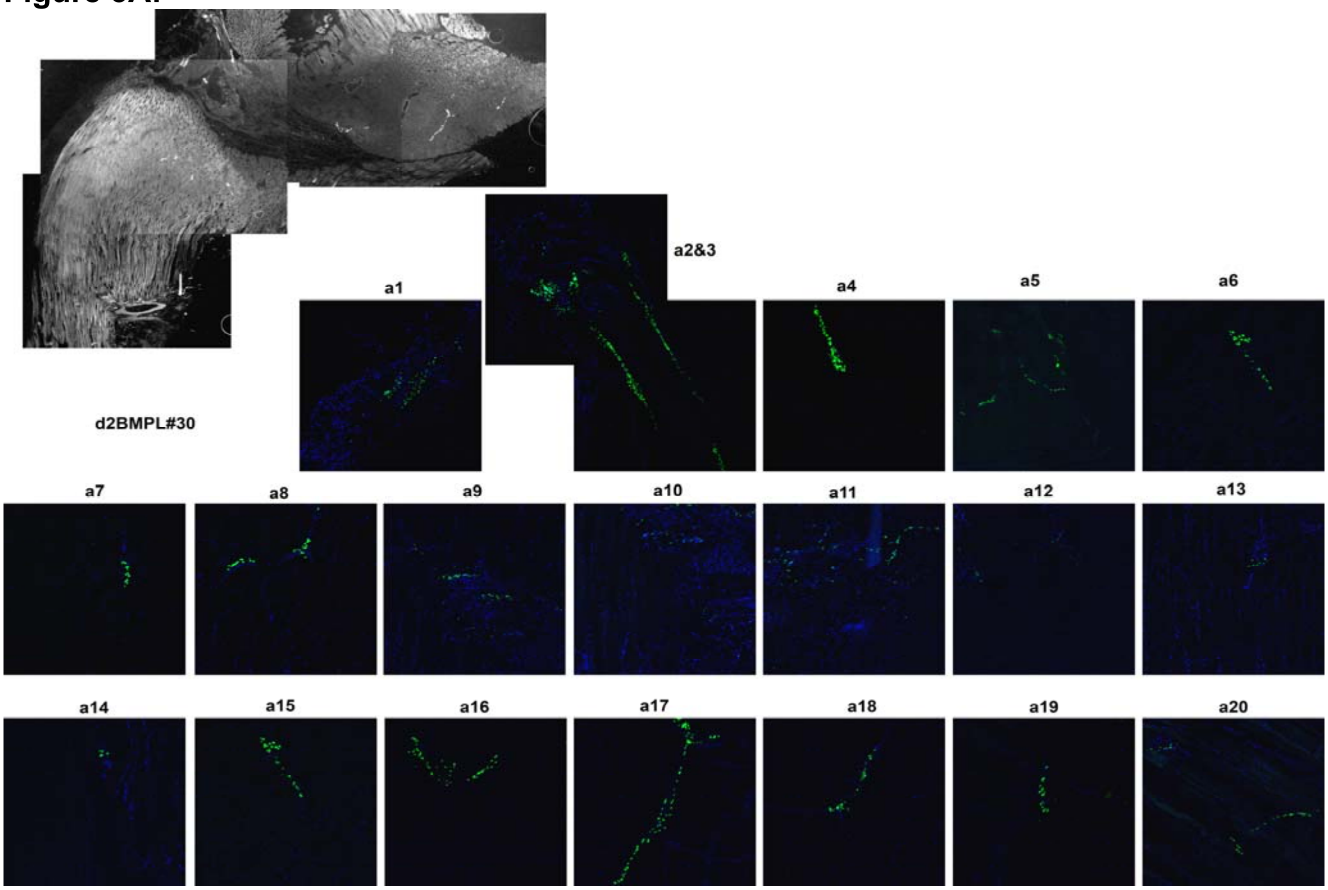
d2BMPL#30
a1
a2&3
a4
a5
a6
a7
a8
a9
a10
a11
a12
a13
a14
a15
a16
a17
a18
a19
a20

Figure 3B:

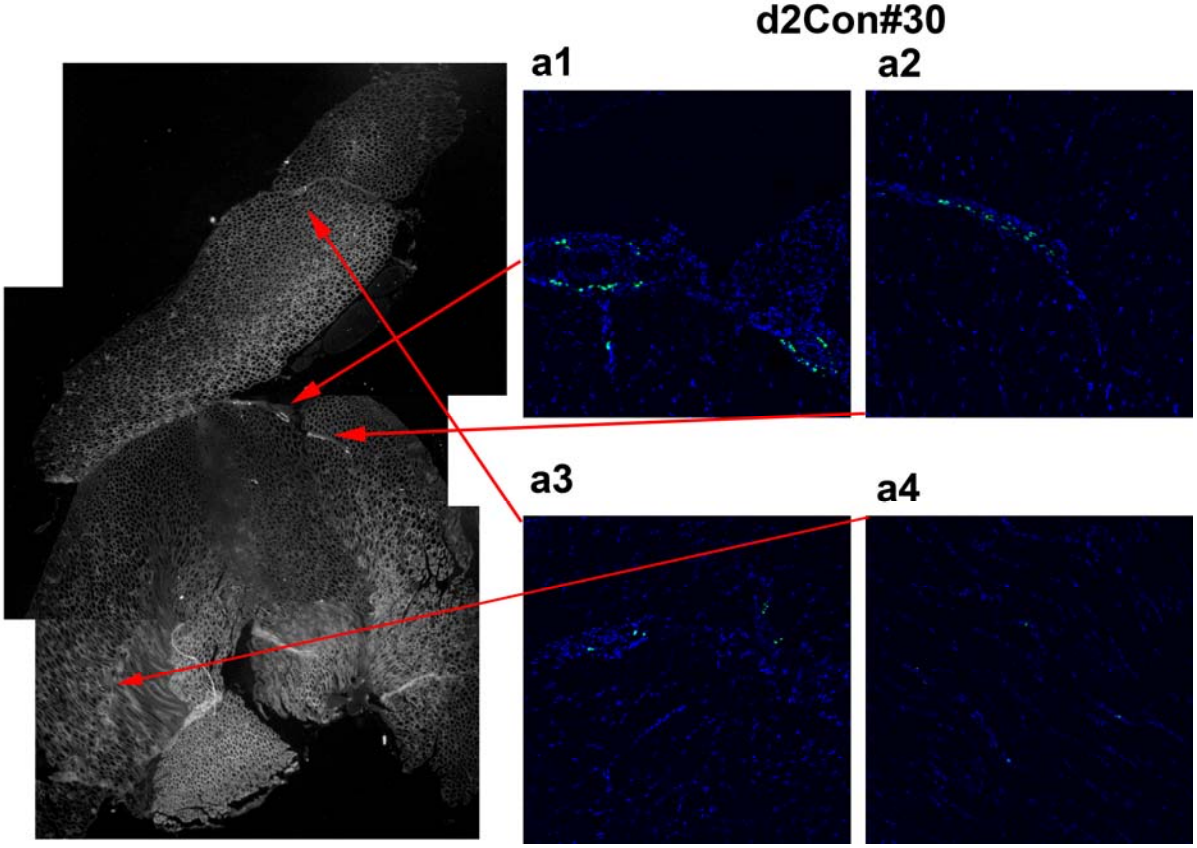

Figure 4A:

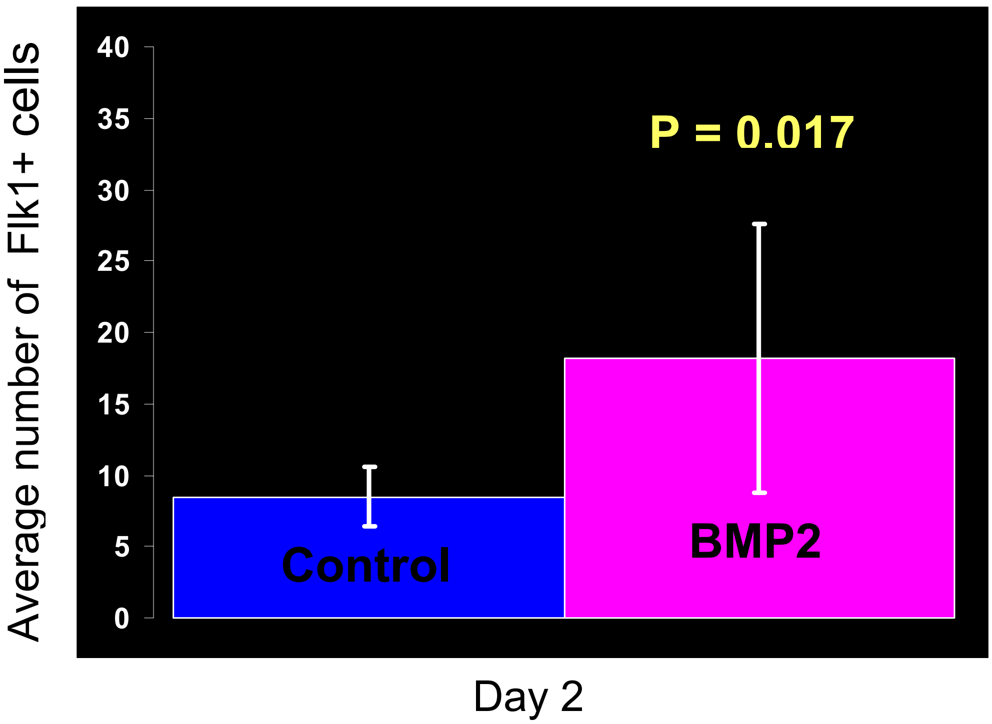
Average number of Flk1+ cells
40
35
30
25
20
15
10
5
0
P = 0.017
Control
BMP2
Day 2

Figure 4B:

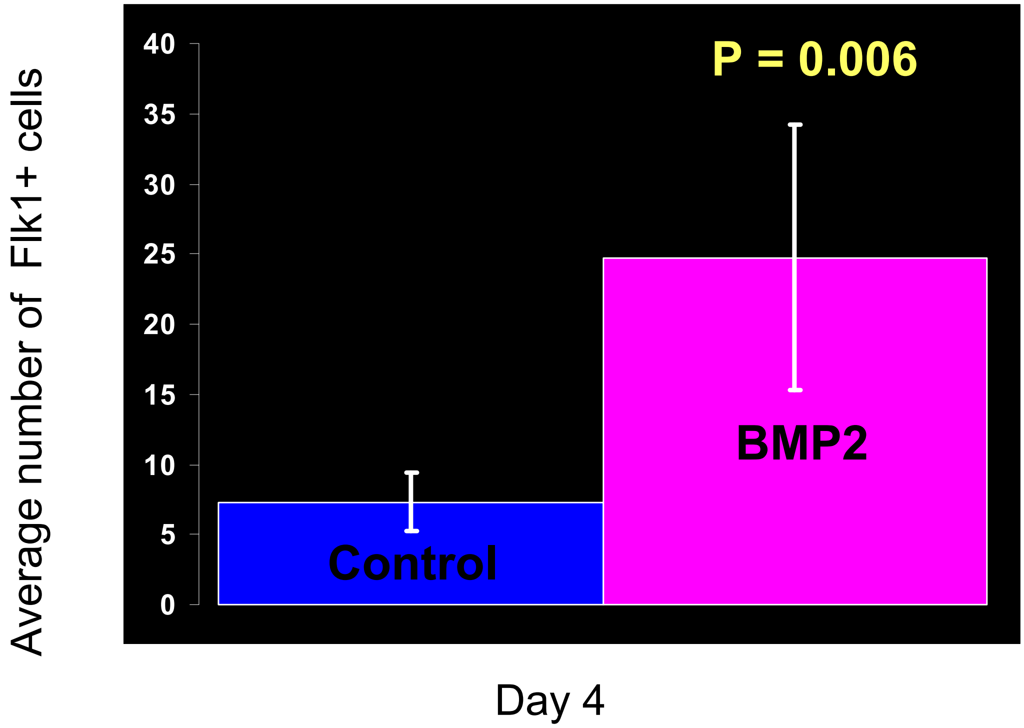
P = 0.006
Average number of Flk1+ cells
40
35
30
25
20
15
10
5
0
BMP2
Control
Day 4

Figure 5A:

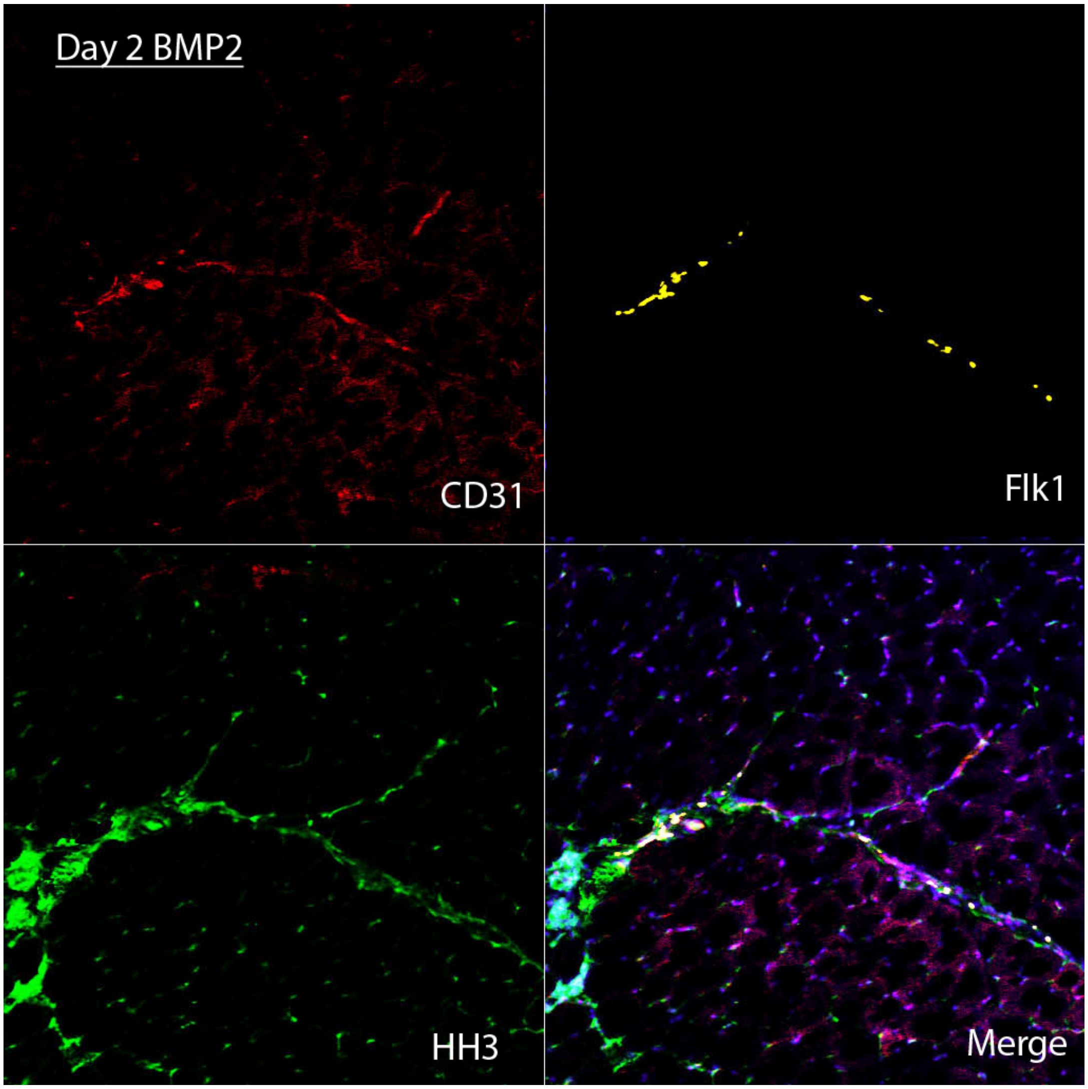

Figure 5B:

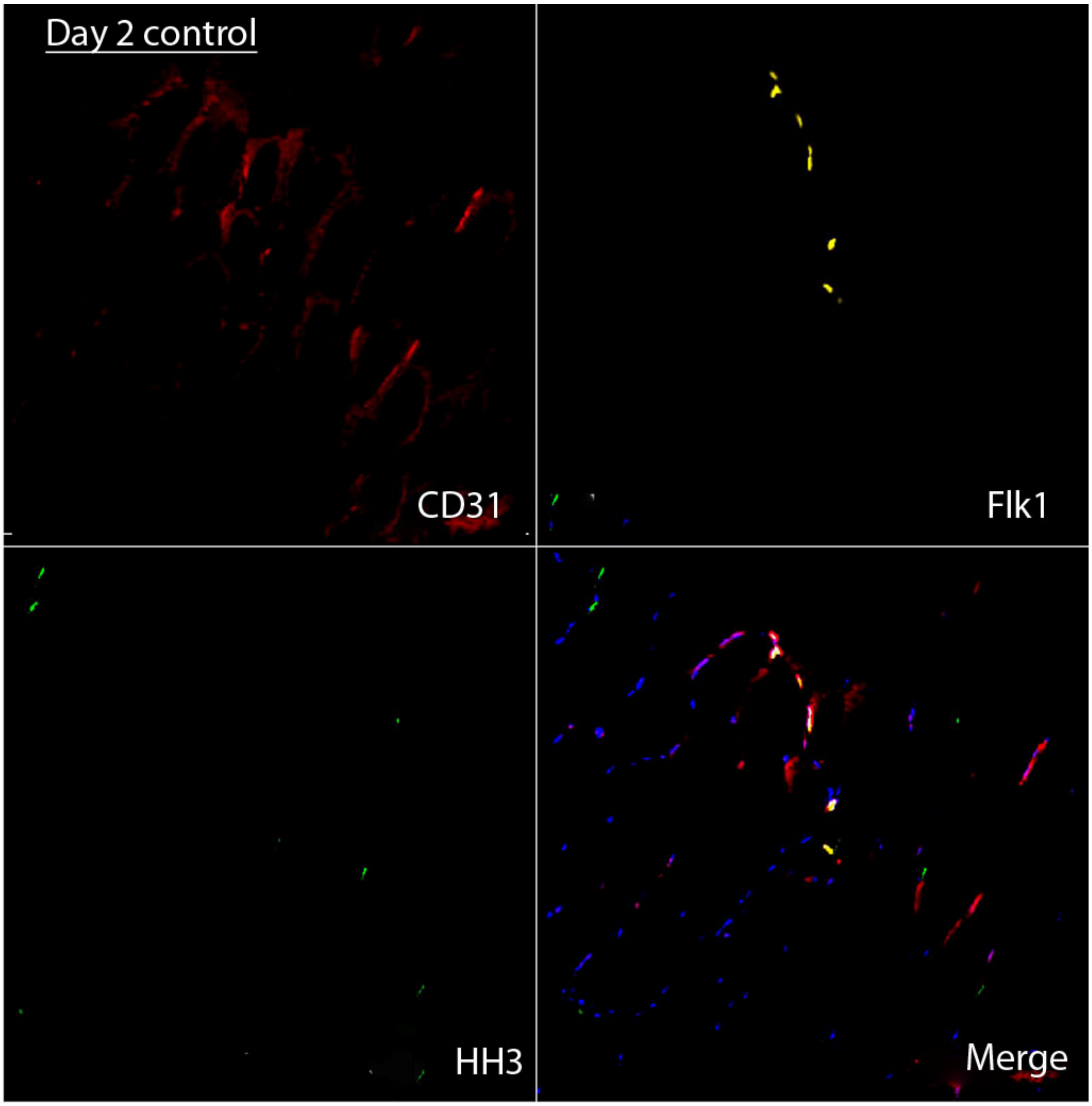

l

Figure 6:

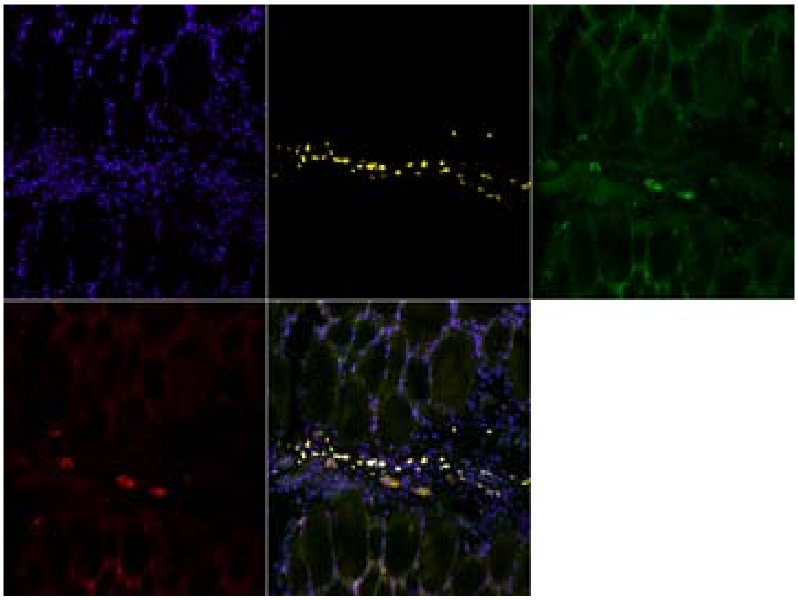

REFERENCES

1. Colnot C, Lu C, Hu D, Helms JA 2004 Distinguishing the contributions of the perichondrium, cartilage, and vascular endothelium to skeletal development. Dev Biol **269**(1)**:**55-69.
2. Maes C, Stockmans I, Moermans K, Van Looveren R, Smets N, Carmeliet P, Bouillon R, Carmeliet G 2004 Soluble VEGF isoforms are essential for establishing epiphyseal vascularization and regulating chondrocyte development and survival. J Clin Invest **113**(2)**:**188-99.
3. Gerber HP, Vu TH, Ryan AM, Kowalski J, Werb Z, Ferrara N 1999 VEGF couples hypertrophic cartilage remodeling, ossification and angiogenesis during endochondral bone formation. Nat Med **5**(6)**:**623-8.
4. Li J, Zhang YP, Kirsner RS 2003 Angiogenesis in wound repair: angiogenic growth factors and the extracellular matrix. Microsc Res Tech **60**(1)**:**107-14.
5. Fouletier-Dilling CM, Gannon FH, Olmsted-Davis EA, Lazard Z, Heggeness MH, Shafer JA, Hipp JA, Davis AR 2007 Efficient and rapid osteoinduction in an immune-competent host. Hum Gene Ther **18**(8)**:**733-45.
6. Olmsted-Davis E, Gannon FH, Ozen M, Ittmann MM, Gugala Z, Hipp JA, Moran KM, Fouletier-Dilling CM, Schumara-Martin S, Lindsey RW, Heggeness MH, Brenner MK, Davis AR 2007 Hypoxic adipocytes pattern early heterotopic bone formation. Am J Pathol **170**(2)**:**620-32.
7. Shen M, Yoshida E, Yan W, Kawamoto T, Suardita K, Koyano Y, Fujimoto K, Noshiro M, Kato Y 2002 Basic helix-loop-helix protein DEC1 promotes chondrocyte differentiation at the early and terminal stages. J Biol Chem **277**(51)**:**50112-20.
8. Fraser ST, Hadjantonakis AK, Sahr KE, Willey S, Kelly OG, Jones EA, Dickinson ME, Baron MH 2005 Using a histone yellow fluorescent protein fusion for tagging and tracking endothelial cells in ES cells and mice. Genesis **42**(3)**:**162-71.
9. Olmsted EA, Blum JS, Rill D, Yotnda P, Gugala Z, Lindsey RW, Davis AR 2001 Adenovirus-mediated BMP2 expression in human bone marrow stromal cells. J Cell Biochem **82**(1)**:**11-21.
10. Fouletier-Dilling CM, Bosch P, Davis AR, Shafer JA, Stice SL, Gugala Z, Gannon FH, Olmsted-Davis EA 2005 Novel compound enables high-level adenovirus transduction in the absence of an adenovirus-specific receptor. Hum Gene Ther **16**(11)**:**1287-97.
11. Olmsted-Davis EA, Gugala Z, Gannon FH, Yotnda P, McAlhany RE, Lindsey RW, Davis AR 2002 Use of a chimeric adenovirus vector enhances BMP2 production and bone formation. Hum Gene Ther **13**(11)**:**1337-47.

12. Gerdes J, Schwab U, Lemke H, Stein H 1983 Production of a mouse monoclonal antibody reactive with a human nuclear antigen associated with cell proliferation. Int J Cancer **31**(1)**:**13-20.
13. Shafer J, Davis AR, Gannon FH, Fouletier-Dilling CM, Lazard Z, Moran K, Gugala Z, Ozen M, Ittmann M, Heggeness MH, Olmsted-Davis E 2007 Oxygen tension directs chondrogenic differentiation of myelo-monocytic progenitors during endochondral bone formation. Tissue Eng **13**(8)**:**2011-9.
14. Sato Y, Kanno S, Oda N, Abe M, Ito M, Shitara K, Shibuya M 2000 Properties of two VEGF receptors, Flt-1 and KDR, in signal transduction. Ann N Y Acad Sci **902:**201-5; discussion 205-7.
15. Trelles RD, Leon JR, Kawakami Y, Simoes S, Belmonte JC 2002 Expression of the chick vascular endothelial growth factor D gene during limb development. Mech Dev **116**(1-2)**:**239-42.
16. Li X, Cao X 2006 BMP signaling and skeletogenesis. Ann N Y Acad Sci **1068:**26-40.
17. Hogan BL 1996 Bone morphogenetic proteins in development. Curr Opin Genet Dev **6**(4)**:**432-8.
18. Rissanen TT, Markkanen JE, Gruchala M, Heikura T, Puranen A, Kettunen MI, Kholova I, Kauppinen RA, Achen MG, Stacker SA, Alitalo K, Yla-Herttuala S 2003 VEGF-D is the strongest angiogenic and lymphangiogenic effector among VEGFs delivered into skeletal muscle via adenoviruses. Circ Res **92**(10)**:**1098-106.

Supplemental data:

To verify that the Flk-H2B::EYFP was restricted to endothelial cells, we first analyzed the normal adult muscle to examine that the Flk-1-H2B::EYFP expressed in the endothelial cells. YFP positive cells appeared to be association with the endothelial cells labeled by antibodies against CD31 and Flk1 (figure1). When endogenous Flk1 positive cells are immunolabled, smaller vessels showed co-localization of YFP and Flk1 positive cells, however, not all the Flk1 positive vessels contained YFP positive cells. Since vascular smooth muscle actin (SMA) is also expressed by cell surrounding vascular endothelial cells, we examined whether the YFP expression is associated with the smooth muscle cells using SMA antibody for immuostaining, and we do see the YFP expression in smooth muscle positive vasculature (figure. 1). From our immunolocalization analysis, the endothelial marker VE-cadherin (data not shown) and CD31 marker also exhibit a similar localization pattern with YFP positive cells (figure. 1, table 1).

Using image analysis software, FARSIGHT (RPI, New York), we performed segmentation analysis on RGB images, where we associated immunostaining signals to the red channel, YFP to the green channel, and DAPI to the blue channel. First, DAPI stained nuclei in the blue channels were segmented using FARSIGHT. The total number of segmented nuclei was defined as the total number of cells. Similarly, YFP positive nuclei in the green channels were segmented and counted as YFP positive cells (figure. 1). The fraction of cells that were immumostaining positive was counted by taking the ratio of DAPI stained nuclei that were immumostaining positive (red channel) to the total

number of DAPI stained nuclei. Then, the immuno-stained positive cells were classified as YFP positive cells and YFP negative cells. Data sets were quantified and described in the table 1. From this analysis, we demonstrated that adult muscle tissue express H2B::EYFP in the endothelial cells, however, they represents a subset of endothelial cells.

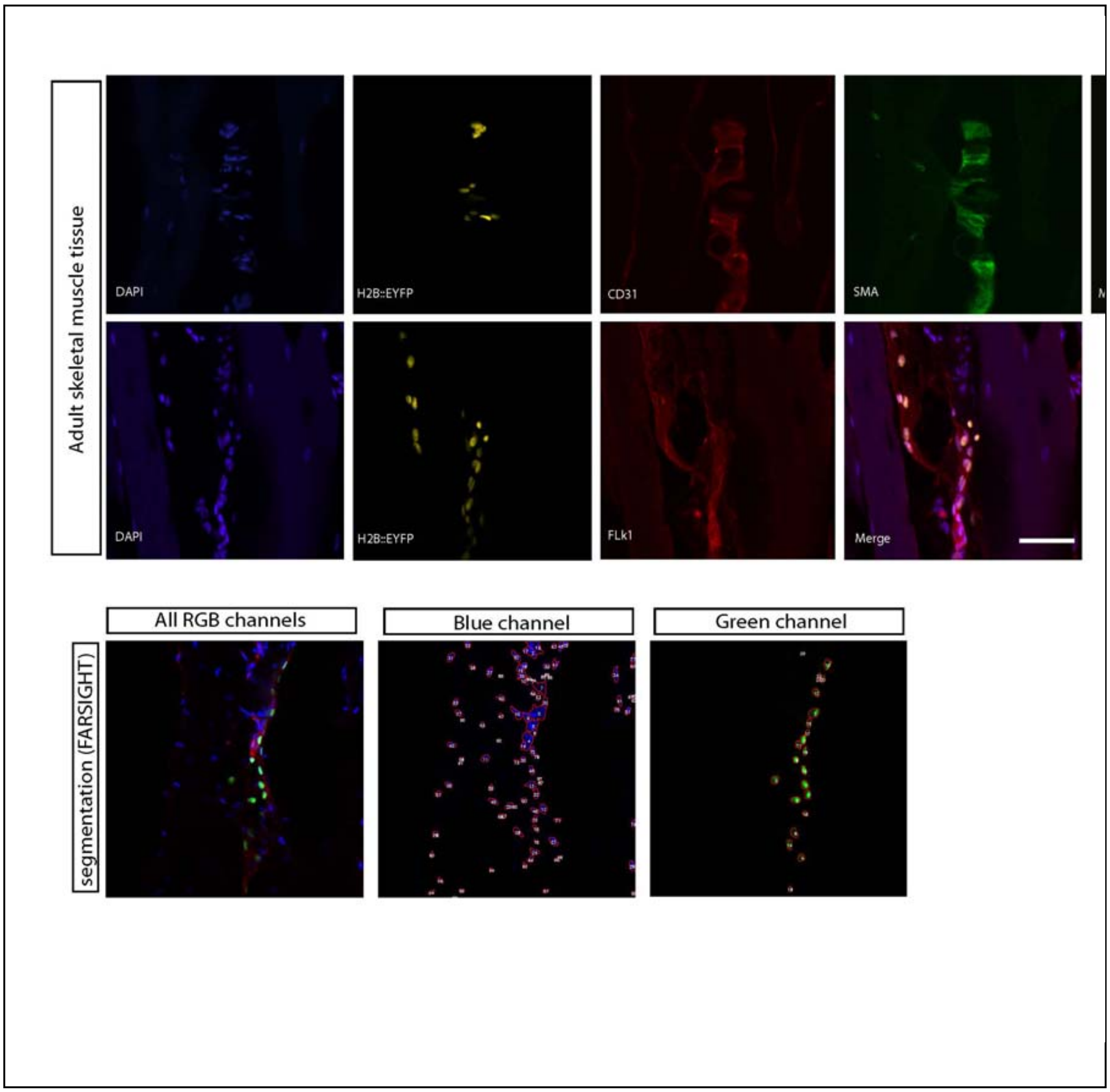

Figure.1

Table.1

CD31 (8 pictures)	CD31+/DAPI+	YFP+ CD31+/YFP+	YFP+ CD31+/CD31+
Mean	84.56%	100.00%	20.74%
Stv	10.87%	†	16.95%
Confident Interval (95%)	7.10%	†	11.07%
VE-Cad (6 pictures)	**VE-Cad+/DAPI+**	**YFP+ VE-Cad +/YFP+**	**YFP+VE-Cad +/VE-Cad +**
Mean	87.67%	100.00%	8.61%
Stv	6.59%	†	3.67%
Confident Interval (95%)	4.31%	†	2.40%

FLK1 (6 pictures)	FLK1+/DAPI+	YFP+ FLK1 +/YFP+	YFP+ FLK1 +/FLK1 +
Mean	94.93%	100.00%	16.94%
Stv	5.22%	†	7.02%
Confident Interval (95%)	4.18%	†	5.61%
SMA (12 pictures)	**SMA +/DAPI+**	**YFP+ SMA +/YFP+**	**YFP+ SMA +/ SMA +**
Mean	62.64%	93.31%	23.53%
Stv	16.71%	10.04%	14.14%
Confident Interval (95%)	13.37%	8.03%	11.32%

All nucleus → DAPI+
DAPI with CD31+ and YFP- →CD31+
DAPI with CD31- and YFP+ →YFP+
DAPI with CD31+ and YFP+ →CD31+YFP+